Enantioselective synthesis of proline derivatives by 1,3-dipolar cycloadditions

Carmen Nájera ● José M. Sansano

Received: ……/Accepted …

Abstract In this account the research devoted to the synthesis of highly substituted prolines, which are hepatitis C viral inhibitors using 1,3-dipolar cycloadditions of azomethine ylides is described. The evolution of our continuous work it will be displayed involving, in a first term, the diastereoselective approach using an inexpensive lactate derived acrylate as dipolarophile. In a second part, it will be described all our efforts using simple and easily accessible chiral silver(I) and gold(I) complexes as catalysts for the enantioselective synthesis of proline derivatives. In this case, chiral phosphoramidites and Binap have been used as privileged ligands. Parallelly to these experimental results, a considerable effort was dedicated to run semiempirical-DFT calculations in order to explain and justify the stereoselection of each process.

Keywords Antiviral activity ● Chiral catalysts ● Azomethine ylides ● Cycloadditions ● Prolines ● Lewis acids

C. Nájera ● J. M. Sansano (✉)

Departamento de Química Orgánica e Instituto de Síntesis Orgánica, Universidad de Alicante, Apdo. 99, 03080-Alicante (Spain)

e-mail: cnajera@ua.es and jmsansano@ua.es

Introduction

Proline Derivatives

Proline **1** or proline derivatives constitute a very important family of natural or synthetic compounds with very interesting chemical and bioactive applications. Proline surrogates are of special interest given the key role of proline in nucleating the secondary structures, and hence the biological behavior, of peptides. These rigid amino acids represent a powerful mean to overcome their shortcommings since a limited conformational freedom often protects from proteolytic degradation and sometimes leads to improved selectivity and potency [1].

Spite of the main importance is probably their use in structure-activity relationship (SAR) studies [1], the synthesis of pyrrolidine core-based natural products [1,2,3] or even the application of these small units as very efficient organocatalysts [4,5] are very productive scientific areas. For example, 4-hydroxyproline **2** (R = H) is the major component of the protein collagen, playing key roles in the increment of collagen stability. (−)-α-Kainic acid **3**, (−)-domoic acid **4**, and acromelic acid **5** belong to a family of kainoid natural neurotoxins, promoting a potent stimulation of the central nervous system, brain damage, and neurological disorders, respectively (Chart 1) [1]. In addition, synthetic molecules **6**-**9** have been identified as potent hepatitis C virus (HCV) inhibitors blocking the viral

RNA-dependent RNA-polymerase [6]. The last proline **9** (GSK 625433), which is now in phase I trials, has shown potent selective activity against type 1a and 1b HCV polymerases (D. Haigh, GlaxoSmithKline, UK). Moreover, proline **1** or its derivatives **2**, **10**, and **11**, are suitable new organocatalysts for asymmetric synthesis [4,5].

<Chart 1>

A number of strategies devised for the synthesis of proline derivatives [1,2,3,7] involve: a) the α-functionalization of L-proline itself or other derivatives; b) the intramolecular cyclizations of chiral amino acids; and c) the formation of the pyrrolidine ring through a 1,3-dipolar cycloaddition (1,3-DC) of azomethine ylides. The last methodology is the most straightforward route for the preparation of highly substituted prolines.

1,3-Dipolar Cyloadditions of Azomethine Ylides

Since the publication of the first example of a 1,3-dipolar cycloaddition by Hüisgen in 1963 [8], many contributions have appeared [9]. In recent years, azomethine ylides have become one of the most investigated classes of 1,3-dipoles due to their cycloaddition chemistry [9,10].

The high reactivity of the azomethine ylides requires their generation in situ, which can be achieved through several routes. Whilst non-stabilized azomethine ylides are considering fleeting intermediates, the stabilized ones **14** or **15** possess higher life times allowing a wider scope of the cycloadditions. Nowadays, iminoesters **13** afford these 1,3-dipoles through a thermal 1,2-prototropy shift process or by a base-promoted enolization followed by intramolecular chelation, respectively (Scheme 1). The last process occurs under very mild reaction conditions and the control of the geometry of the resulting metallo-dipole is extremely high. This feature, together with the frontier orbital theory (FOT)-justified regioselectivity, and the high *endo*- or *exo*-diastereoselection observed, make this generation of the 1,3-metallodipoles much more attractive and useful in this particular organic synthetic area. The reaction of the dipole with the electrophilic alkene to give **16** occurs through a concerted process under thermal conditions, and, probably, via a stepwise manner (a Michael type addition reaction followed by intramolecular cyclization) when a 1,3-metallodipole **15** is involved [10].

<Scheme 1>

The standard 1,3-dipolar cycloaddition of stabilized azomethine ylides **18**, easily prepared from iminoesters **17**, occurs with high-LUMO alkenes under very mild reaction conditions affording *endo*- or *exo*-cycloadducts **19** (Scheme 2). Stereoelectronic effects control the *endo/exo* ratio of the final product **19**. These *endo* and *exo* notations concern the two different approaches of the dipolarophile to the metal center. The *endo*-approach occurs when the electron-withdrawing group (EWG) that induces the Michael-type addition step is very close to the metal cation favoring a very weak coordination between them (*endo*-TS **20** in Scheme 2). However, in the *exo*-approach the EWG is oriented far away from the metal center such as it is depicted in *exo*-TS **21** in Scheme 2.

<Scheme 2>

The 1,3-DC becomes extremely useful when all these aspects are focused on the design of an asymmetric process [10]. On it, the generation of up to four stereogenic centers can be unambiguously created in just one reaction step. Currently, the non-racemic 1,3-DC can be efficiently achieved through diastereoselective strategies by employing chiral azomethine ylides or chiral dipolarophiles, and secondly, via enantioselective processes using chiral catalysts.

In this account, we will describe the evolution of our research on the development of asymmetric methodologies for the synthesis of biologically active HCV inhibitors **6-8**. Parallelly, a wide study of the general scope of each of them will be also introduced.

Results and Discussion

Diastereoselective methods

In optically active azomethine ylides, the chiral information can be located at the EWG or at the imino group, however, it has been described chiral α-amino acid templates **23-25** as azomethine ylide precursors where the chiral domain was directly bonded to both functional imino and electron-withdrawing groups. The most recent reported chiral azomethine ylides are those derived from amines **22-25 [**11**]** (Chart 2) and aldehydes upon heating. In all cases, good chemical yields and moderate to good diastereoselections were obtained. At the end of the process the chiral auxiliary must be separated from the pyrrolidine moiety. In this sense, for example, the Oppolzer's sultam fragment of precursor **22** could be easily recoverable under mild reaction conditions yielding enantiomerically pure proline derivatives. By contrast, the chiral auxiliary was not removed in the case of the chiral iminoester **26** [12], which was the precursor of the silver

metallodipole and, after completing the corresponding cycloaddtion, the chiral β-lactam unit was employed for the construction of more complex structures.

<Chart 2>

In other side, chiral electrophilic alkenes can be alternatively employed. In this option, the most recent examples anchored the chiral information as substituent of the carbon-carbon double bond such as occurred in molecules **27 [**13**]** and **28 [**14**]**, or at the electron-withdrawing group as, for example, in molecules **29-33** [15] (Chart 3).

<Chart 3>

Enantiomerically enriched acrylates (*R*)- and (*S*)-**34**, employed in diastereoselective Diels-Alder reactions, in the synthesis of natural products and complex heterocycles [16], were envisaged as chiral dipolarophiles in the diastereoselective 1,3-DC. Firstly, we improved the synthesis of these enantiomerically enriched alkenes in a simple process involving the esterification of the chiral lactic acid with acryloyl chloride in the presence of triethylamine and substoichiometric amounts of *N*,*N*-

dimethylaminopyridine (DMAP) [17]. This new procedure avoided the employment of toxic and no longer commercially available carbon tetrachloride.

The 1,3-DC of (*S*)-**34** with metallo-azomethine ylides, derived from iminoesters **35**, efficiently proceeded under mild reaction conditions obtained after an optimization protocol, that means, AgOAc (10 mol%), KOH (10 mol%) as base, in toluene at room temperature for 1d (Scheme 3). For glycine-derived 1,3-dipoles, the influence of the ester group could be observed when the benzaldehyde iminoglycinates **35** (R^1 = H, R^3 = Ph, 2-Naphthyl) were allowed to react with the chiral alkene (*S*)-**34** (Table 1, entries 1-5). The reactions proceed quantitatively and the best diastereoselections were achieved when the *t*-butyl esters were employed. It was also noticeable the higher diastereoselections exhibited by the methyl esters versus the analogous transformations performed with the isopropyl esters. Several α-substituted amino acids such as alanine, phenylalanine, and leucine were used for the elaboration of the 1,3-dipole. In the reactions carried out with these α-branched 1,3-dipole precusors there was not a very significant difference, in terms of diastereoselection, between using methyl or *t*-butyl esters (see for instance, Table 1, compare entries 6 and 7). So, all the reactions were performed in 2 days with the corresponding methyl esters affording, in all cases good chemical yields

and good to excellent diastereoselectivities of the *endo*-cycloadducts **36**, especially for the reaction involving the phenylalanine derivative (R^3 = 2-thienyl) (Table 1, entry 9). This excellent result encouraged us to design the key step for the non-racemic synthesis of the first generation of antiviral agent **6**. The reaction of the methyl, isopropyl or *t*-butyl iminoleucinates (R^1 = Bu^i, R^3 = 2-thienyl) with the acrylate (*S*)-**34** occurred under the standard reaction conditions affording good chemical yields and very good diastereoselections of the cycloadduct **36** (Table 1, entries 10-12). Once more the methyl ester derivative was the most appropriate substrate, rather than isopropyl or *t*-butyl esters. In all of these examples the *endo*/*exo* ratio observed by ^{1}H NMR spectroscopy was higher than 98/2.

<Scheme 3>

<Table 1>

The absolute configuration of the *endo*-products **36** could be determined by X-ray diffraction analysis of the *N*-tosylated cycloadduct **37**, showing that the *S*-absolute configuration of the lactate moiety induced a 2*R*,4*R*,5*S*-configuration in the pyrrolidine ring (Scheme 4).

<Scheme 4>

According to this stereochemical arrangement the acrylate (*S*)-**34** would be valuable for the synthesis of (−)-**6**, whilst enantiomeric acrylate (*R*)-**34** would serve for the preparation of biologically more active compound (+)-**6**, although the activity of the racemic form is not negligible (Chart 4). For this reason, we firstly undertook the synthesis of antiviral agent (±)-**6** such as it is shown in Scheme 5. The non-isolated cycloadduct obtained from the iminoester **35** (R^1 = Bu^i, R^2 = Me, R^3 = 2-thienyl) and methyl acrylate in the presence of AgOAc (10 mol%), was allowed to react with 4-(trifuromethyl)benzoyl chloride in DCM for 2 days yielding the corresponding amide **38** in 88% yield. The final product (±)-**6** was isolated in 68% yield after a combined hydrolytic process based on a treatment of tributyltin hydroxyde required for the elimination of the chiral auxiliary, followed by a reflux of a 1M KOH/MeOH solution for the hydrolysis of the ester group placed at the α-position of the proline (Scheme 5).

<Chart 4>

<Scheme 5>

The synthesis of non-racemic antiviral agents was not reported before these research studies, but the enantiomerically enriched samples were obtained through semi-preparative chiral HPLC [18]. The preparation of both enantiomers (+)- or (−)-**6** was achieved using a very similar route starting from the iminoester **35** (R^1 = Bu^i, R^2 = Me, R^3 = 2-thienyl) an the more expensive acrylate (*R*)-**34** or the unexpensive acrylate (*S*)-**34**, respectively. These key steps afforded the *endo*-cycloadduct **35** in 77-78% chemical yields and 96% *de* (Table 1, entry 10). The amidation reaction and the double hydrolytic processes were identical to those described for the synthesis of the racemic antiviral agent (Scheme 6) obtaining an overall yield of 68% from the cycloadduct **36**.

<Scheme 6>

In order to understand the origins of this excellent regio- and stereocontol observed by this small chiral environment, DFT calculations were carried out [17b]. Based on a previous computational work determining that these 1,3-DC occur in a non-concerted but stepwise mechanism [19], and the structure of the catalytic metal complex (AgOAc in the presence of KOH), four transition states (Figure 1) were optimized.

The absence of an additional ligand/anion to the silver cation (in this case water is included) promoted a key coordination between the meal and two carboxylate groups which favored the *endo*-approach with the experimentally obtained stereochemistry.

<Figure 1>

Enantioselective methods

The enantioselective approach is very advantageous because the elimination of the chiral auxiliary is not required, and additionally, only a tiny amount of the chiral catalyst is enough for the achievement of a large enantioselection [10k]. Particularly, the 1,3-DC of metallo azomethine ylides and alkenes was pioneered by Grigg and coworkers in 1991 using stoichiometric amounts of chiral bases or chiral metal complexes [20]. However, it was just in 2002 when the first substoichiometric catalytic (3 mol%) enantioselective transformation was successfully reported by Zhang and coworkers using a chiral diphosphane/silver(I) complex [21]. At that time, this cycloaddition became a fascinating transformation and many contributions appeared with outstanding results. Chiral metal complexes, chiral bases, and chiral organocatalysts have all given excellent results, in terms of diastereo- and enantioselectivities, and wider general scope when

chiral metallodipoles were generated as intermediates. Based on the previous results obtained with silver(I) [22] and copper(I) [23], it has been published a series of catalytic chiral complexes. The most representative recent silver(I) complexes are depicted in Chart 5 generating the corresponding *endo*-diastereoisomer as major reaction product [24], whilst in Chart 6 the most relevant chiral copper(I) are displayed, which exhibited not so defined sterereoselection such as silver(I) complexes did [25]. Other different metal cations have also been employed affording exclusively the *endo*-cycloadducts (Chart 7) [26]. All of these example were carried out employing α-iminoesters as 1,3-dipole precursors except the reactions dealing with azlactones and electrophilic alkenes catalyzed by the chiral **53**-gold(I) complex [26e]. Apart of these catalytic enantioselective 1,3-DCs involving α-iminoesters, the generation of stabilized metallo-1,3-dipoles has been achieved starting from α-iminophosphonates using chiral silver(I) complexes [27] and α-iminonitriles employing chiral copper(I) complexes [28].

<Chart 5>

<Chart 6>

<Chart 7>

Organocatalysts have also been successively applied to these cycloadditions [29] however, they and the chiral metal complexes have completely different behaviours concerning the 1,3-dipole and dipolarophile. Organocatalysts, unless that their basicity is relatively high, require a very activated arylideneiminomalonate as 1,3-dipole precursor, and in many cases, its successful enantioselective process is limited to one dipolarophile. In this sense, structural limitations are notable and there are not wide-scope transformations at the moment. By contrast, the chiral metal complex-catalysed enantioselective approach has been much more studied and the structural limitations are minimal, finding very interesting broad scopes for several chiral metal complexes.

Taking in account all these details, and continuing with our research focussed on the preparation of namely antiviral agents, we select the enantioselective 1,3-DC mediated by a chiral Lewis acid able to afford, in a reliable manner, the relative *endo* configuration of the target key molecules. Silver(I) salts were the most appropriate at the beginning and we choose easily available chiral ligads such as phosphoramidites **42** and **43** and Binap **44** (Chart 8).

<Chart 8>

Although chiral phosphoramidites **42** and **43** [30], (Figure 1) have been extensively used in asymmetric hydrogenations and many other transformations such as allylations, Michael-type additions, and carbonyl addition reactions [31], they were not previously used as ligands in 1,3-DC between azomethine ylides and dipolarophiles. We envisaged that a monodentate ligand would favor the formation of a very highly-congested transition state. Initially, the optimization of the reaction was carried out at room temperature employing *tert*-butyl acrylate and methyl *N*-benzylideneimino glycinates **35** (R^1 = H, R^2 = Me, R^3 = Ph). Employing 5 mol-% of catalyst, formed by in situ addition of a 1:1 mixture of phosphoramidite **43** and the silver perchlorate, in the presence of triethylamine as organic base (5 mol-%) afforded the best enantioselections of **45** at −20 ºC. The catalysts formed by $AgClO_4$ (5 mol-%) and ligand (S_a)-**42** (5 mol-%) and triethylamine as base (5 mol-%) gave lower *er* of the corresponding cycloadduct. When a 2:1 mixture of $AgClO_4$:(S_a,*R*,*R*)-**43** (5 mol-%) was used instead the *er* was also lower than the result described for the 1:1 mixture. As well, the matching configuration S_a,*R*,*R* of the chiral ligand was confirmed for this particular example of cycloaddition [32].

In this the first enantioselective 1,3-DC of azomethine ylides and alkenes using monodentate ligands, these unknown complexes were characterized by X-ray crystallographic diffraction of monocrystals. Whilst the 1:1 (S_a,*R*,*R*)-**43**:$AgClO_4$ complex formed cross-linked sheets, the 2:1 mixture afforded well defined crystals (Figure 2). The formation of these polymeric assemblies are typical of silver(I) complexes, independently of the mono- or bidentate character of the corresponding ligand [33].

<Figure 2>

The ESI-MS experiments of the 1:1 and 2:1 (S_a,*R*,*R*)-**43**:$AgClO_4$ complexes revealed M^++1 peaks at 646 and 1187, respectively. When an equimolar amounts of the 1,3-dipole precursor **35**, triethylamine, and a 1:1 mixture of (S_a,*R*,*R*)-**3**:$AgClO_4$ complex were put together, the ESI experiment revealed a very abundant species with *m/z* = 824, due to the formation of the chiral silver complex-dipole adduct **I** (Figure 3) and a tiny peak at 1000 as a result of the combination of two molecules of dipole to the chiral silver complex.

<Figure 3>

^{31}P NMR ($CDCl_3$, 10 mol-% aq. polyphosphoric acid as internal reference) experiments also revealed interesting aspects. Only a wide band centered at 126.9 ppm was observed when a 1:1 mixture of (S_a,*R*,*R*)-**43**:$AgClO_4$ was formed in solution, which corresponded to its polymeric character detected by X-ray diffraction analysis. However, two separated bands were observed at 124.9 and 132.0 ppm in the case of a 2:1 mixture as a consequence of the partial disaggregation. The almost complete disaggregation of the polymeric sheets of the 1:1 complex was achieved with the addition of 1 equiv. of the 1,3-dipole generate from **35** and triethylamine. The result was the transformation of the original ^{31}P NMR band into two perfectly defined doublets at 125.1 ($J_{P\text{-}Ag(109)}$ = 76 Hz) and 133.61 ppm ($J_{P\text{-}Ag(107)}$ = 73 Hz), which, seems to correspond to the phosphorous atom of the complex **I**.

Due to perchlorates are classified as low order explosives the thermal stability of the 1:1 mixture of (S_a,*R*,*R*)-**3**:$AgClO_4$ complex was studied. The thermogravimetric (TG) and differential thermal analysis (DTA) of this complex revealed that the loss of water occurred from 50 to 150 ºC without any variation of the heat of the system. The exothermic decomposition of the complex started at 200 ºC approximately, continuing till 600 ºC with a noticeable heat liberation.

The scope of the reaction can be observed in the results described in Table 2 operating with methyl or isopropyl iminoesters because *tert*-butyl esters did not complete the reaction properly. Isopropyl esters were good starting materials for this enantioselective cycloadditions, especially when phenyl or 4-substituted aryl iminoglycinates were employed, although methyl esters were more appropriate for the sterically hindered 2-substituted aryl imino groups (Table 2, entries 1-6). For α-substituted 1,3-dipole precursors, the reaction with methyl esters afforded very interesting results. Alanine, phenylalanine, and leucine derivatives afforded high enantioselections and good chemical yields (Table 2, entries 7-10), which was a promising result to access finally the desired antiviral framework.

<Scheme 7>

<Table 2>

Different dipolarophiles were allowed to react with several iminoesters (Scheme 8). Glycine derived iminoesters reacted in very good yields with maleimides at higher temperatures (rt or 0 ºC) obtaining excellent enantioselectivities of the corresponding cycloadducts **46**. Fumarates, chalcone and cyclopent-2-enone were very suitable

dipolarophiles employing triethylamine as base at –20 ºC. The yields of compounds **47**-**49** were in a 72-81% range and the enantioselections were very important, especially in the examples run with chalcone (>99:1 *er*).

α-Substituted iminoesters derived from alanine, and phenylalanine reacted with *N*-methylmaleimide (NMM) furnishing good yields of cycloadducts **46** and high enantiomeric ratios under the analogous reaction conditions, phenylalanine derivative being the less reactive system. Chalcone also reacted with alanine dipole precursor giving good yields of proline derivative **49** (Scheme 8). In all these examples the *endo*:*exo* ratio was higher than 98:2 according to ^{1}H NMR spectroscopy performed to crude reaction products.

<Scheme 8>

Such as it was explained in the previous section, enantiomerically pure proline derivative *endo*-**45** (R^1 = Bu^i, R^2 = Me, R^3 = 2-thienyl) is the key precursor to a series of antiviral agents inhibitors of the hepatitis C virus (HCV) polymerase **6**. The intermediate prolinamide **50** was synthesized in 88% yield (estimated by ^{1}H NMR) from enantiomerically pure *endo*-**45** by a simple amidation reaction with 4-(trifluoromethyl)benzoyl chloride in refluxing dichloromethane during 19

h. The crude product was submitted, in a second step, to a hydrolysis of the *tert*-butyl ester with trifluoroacetic acid followed by the methyl ester hydrolysis using an aqueous solution of KOH in methanol for 16 h. The resulting dicarboxylic acid **6** was finally obtained in 81% yield from compound **50** (50% overall yield from iminoester **35**) (Scheme 9). The purity of the antiviral agent was >98% and only 0.7 ppm of silver were present in this sample according to inductively coupled plasma mass spectrometry (ICP-MS) analysis. On the basis of this instrumental technique, purified samples of compound **45** only contained around 4 ppm of silver.

<Scheme 9>

Apart from the Lewis acid-catalysed 1,3-DC the concept of organocatalysis was applied to the synthesis of **6** using hydroquinine as quiral base (6 mol%) together with a 3 mol% amount of silver acetate. Although chemical yields were very important, the enantioselection was moderate (74% *ee*) (Scheme 11, and Table 1, entry 4). In fact, a further 1,1'-binaphthyl-2,2'-dihydrogen phosphate asisted chiral resolution of **6** was performed in order to obtain pure compound *endo*-**6** with a 99.8% *ee*

[34]. Another similar approach, but using chiral calcium complexes, were published after our seminal contribution [26c].

Calculations located and characterized the four possible transition structures. The less energetic saddle points are those that exhibit the *t*-butoxycarboxyl group in an *endo* relationship with respect to the phenyl group of **35** (R^1 = H, R^2 = Me, R^3 = Ph), exhibiting *ca.* 10 kcal/mol lesser than their *exo*-analogues.

The two possible *endo*-**TS1** saddle points were much closer in energy (Figure 4). However, **TS1-SSR** was calculated to be 1.31 kcal/mol lower in energy than **TS1-RRS** (Figure 4). It is observed that the dihedral angle formed by the two naphthyl groups is of *ca.* 57-58 deg. In the case of **TS1-SSR**, this lead to the blockage of the *Re*-*Si* face of the dipole. Since there is a stronger steric congestion between one naphthyl group and the *tert*-butyl group of the dipolarophile in **TS1-RRS** (Figure 4). This results, in the preferential formation of the *endo*-(2*S*,4*S*,5*R*)-**45,** were in good agreement with the experimental results.

<Figure 4>

At that point, the complex formed by chiral phosphoramidite **43** and silver perchlorate (1:1 mixture) was able to promote the already mentioned

key step to access enantiomerically enriched first generation GSK antiviral agents. However, the analogous reaction employing the methyl iminoleucinate derived from 2-thiazolecarbaldehyde and *tert*-butyl acrylate afforded very poor enantioselections of the key intermediate precursor of chiral pyrrolidine **7**. Alternatively, in parallel studies, we were surveyed the applications of chiral Binap **44**-silver(I) complexes as catalysts in the enantioselective 1,3-DC with the goal of synthesizing the second generation agents, and also for improving the enantioselecivity of the first generation antiviral **6**.

In the publication of the first enantioselective 1,3-DC, by Zhang and co-workers, it was described that the combination of (*S*)-Binap-AgOAc showed low *ee* when dipoles derived from iminoesters **35** were allowed to react with dimethyl maleate (up to 13% *ee*) [21] or with phenyl vinyl sulfone (up to 26% *ee*) [25d,g]. Fortunately, during our screening process, we realized that the model reaction between iminoester **35** (R^1 = H, R^2 = Me, R^3 = Ph) and NMM in toluene at room temperature afforded exclusively *endo*-cycloadduct **46** (R^1 = H, R^2 = Me, R^3 = Ph) with very good enantioselections [35]. After the optimization protocol, we concluded that the best reaction conditions were, once more, toluene as solvent, Et_3N (5 mol%) as base, and a catalytic complex formed by a 1:1 mixture of (*S*)-Binap **44** (5 mol%):silver perchlorate (5 mol%) (Scheme 10).

<Scheme 10>

Unlike the previously described new phosphoramidite-silver(I) complexes, the chiral Binap-silver(I) complexes were known. Complexes formed from silver triflate and (*R*) or (*S*)-Binap **44**, were isolated at different temperatures and further characterized by X-ray diffraction analysis by Yamamoto's group [36]. These studies revealed that mixture of structures **51**-**53** are in equilibrium and at room temperature, being the 1:1 complex **52** the most abundant system (Chart 9).

<Chart 9>

In spite of equimolar [(*S*)-Binap]-$AgClO_4$ and [(*S*)-Binap]-AgOAc complexes gave identical chemical yields of product *endo*-**46** (R^1 = H, R^2 = Me, R^3 = Ph) and very high enantioselection (>99 and 99% *ee*, respectively) the presumed major complex **54** was much more insoluble in toluene than the analogous formed by AgOAc. This property allowed the separation of the complex **54** from the reaction mixture by simple filtration. Surprisingly, complexes (*R*)- and (*S*)-**44**-$AgClO_4$ exhibited a high stability and any apparent decomposition occurred upon the light exposure. Both

complexes **54** and **55** (Chart 10) were prepared and isolated by reaction with 1 and 2 equiv of (*R*)- or (*S*)-Binap together to 1 equiv. of $AgClO_4$, respectively. The mixture was stirred for 1h at room temperature and the complexes were obtained in quantitative yield. Complex (*S*)-**54** was further characterized by ESI-MS experiments showing an M^++1 signal at 731 and a tiny one at 1353. In the case of complex (*S*)-**55**, the same experiment revealed a peak at 1353 and a very small one at 731. However, these two *in situ* formed Binap complexes **54** and **55** could not be differentiated by ^{31}P NMR spectroscopy. Unfortunately, we could not obtain appropriate crystals for their comprehensive and definitive characterization by X-ray diffraction analysis.

<Chart 10>

Again, the thermogravimetric (TG) and differential thermal analysis (DTA) of the stable species **54** were studied. The integrated TG-DTA plot revealed that the loss of water of the sample occurred from 50 to 180 ºC without any variation of the heat of the system. The melting point of this complex **54** is placed in the range of 209-211 ºC. The three most important exothermic decomposition processes occurred approximately at 300, 550 and 860 ºC.

Such as it was described before, the easy separation of the most active major complex (*S*)-**54** was a very important feature to apply in a larger scale process. So, in the reaction between iminoester **35** (R^1 = H, R^2 = Me, R^3 = Ph) and NMM in toluene at room temperature a series of cycles were run employing the same catalytic mixture (1:1 **44**-$AgClO_4$), which was recovered and reused without any additional purification (Scheme 10 and Table 3). The reaction shown in Scheme 10 was performed on a 1 mmol scale on **35** with a 10 mol% of catalyst to facilitate its manipulation and successive reutilization. In the cycles 1- 4 the enantioselectivity was higher than 99% *ee* keeping identical chemical yields (81-91%) (Table 3, entries 1-4). The fifth cycle also afforded the title product *endo*-**46** (R^1 = H, R^2 = Me, R^3 = Ph) in high yield but with a slightly lower *ee* (98%) (Table 3, entry 5) due to the effect of the possible impurities contained in the catalyst. In all of the five cycles tested the *endo*:*exo* diastereoselectivity was higher than 98:2 according to ^{1}H NMR experiments.

<Table 3>

The scope of the reaction employing different aryl- and ester groups at the iminoester **35** structure with assorted dipolarophiles, was next investigated. Several ester and aryl groups were appropriate substituents in

iminoglycinates **35** to perform efficiently the 1,3-DC with maleimides (Scheme 11 and Table 4). Non-substituted methyl arylimino-glycinates **35**, derived from benzaldehyde and 2-naphthalenecarbaldehyde, were the best substrates affording >99% *ee* rather than the ethyl, isopropyl, and *tert*-butyl esters (Table 4, entries 1-5). In these examples, it was also observed that larger amounts of the *exo*-diastereoisomer were formed according to ^{1}H NMR spectroscopy and chiral HPLC. In the reaction performed with catalytic complex (*R*)-**44**, the corresponding enantiomer (2*S*,3*R*,4*R*,5*R*)-*endo*-**46** was obtained. More sterically hindered iminoglycinates derived from *ortho*-substituted aromatic aldehydes gave lower enantioselections (Table 4, entry 6), even working at 0 or –20 ºC and with other bases different to Et_3N, such as DBU or DIEA. Using Et_3N as base, the imines derived electron-withdrawing *para*-substituted aromatic aldehydes furnished high enantioselections (Table 4, entry 7). Heteroaromatic iminoglycinate bearing a 2-thienyl group furnished *endo*-cycloadduct **46** with 92% *ee* after recrystallization (Table 4, entry 8). The recovery of the complex (*S*)-**54** was successfully attempted in the examples recorded in entries 5, 7 and 9 of the Table 4 in 88-93% yield by simple filtration.

Several maleimides were essayed employing the model reaction described in Scheme 11. *N*-Ethylmaleimide afforded similar results of

endo-**46** to the analogous obtained with NMM after 8 h of reaction (Table 4, entry 9). Nevertheless, the bulkier *N*-phenylmaleimide (NPM) furnished lower *ee* (62%) of *endo*-**46** and lower diastereoselectivity (90:10 *endo*:*exo* ratio) (Table 4, entry 10).

Next, sterically hindered α-substituted benzaldimino esters were tested as substrate in this 1,3-DC with NMM. Methyl benzylidenealaninate, methyl phenyliminophenylalaninate and methyl 2-thienyliminoleucinate reacted with NMM under the same reaction conditions at room temperature for 48 h (Table 4, entries 11-13). Cycloadducts *endo*-**46** were diastereoselectivity obtained (>98:2 *endo*:*exo* ratio) and with good enantioselections (72-76% *ee*).

<Scheme 11>

<Table 4>

The absolute configuration of the heterocycle (2*R*,3*S*,4*S*,5*S*) *endo*-**46** (R^1 = Me, R^2 = Me, R^3 = Ph, R^4 = Me) (was determined X-ray diffraction analysis (Figure 5). 2-Thienyl derivatives can be considered as structurally related precursors of active inhibitors of the virus responsible of the hepatitis C.

<Figure 5>

Dipolarophiles different to maleimides were not appropriate for the particular requirements of this enantioselective 1,3-DC catalyzed by the in situ generated complex (*S*)-**54** (Scheme 12). Acrylates, diisopropyl fumarate, and dimethyl maleate gave very high reaction conversions but the enantioselections never exceeded of the 36% *ee* (Scheme 12) maintaining the high *endo*:*exo* diastereoselection.

<Scheme 12>

In order to get a better understanding of the behaviour of these chiral catalysts, we have carried out DFT calculations [35b]. The chief geometric features of complex (*S*)-**A** are gathered in Figure 6. The azomethine ylide part of (*S*)-**A** shows different distances for the two C-N bonds. These distances are compatible with an iminium-enolate structure as shown in Scheme 13, thus anticipating quite asynchronous transition structures in the reaction with the dipolarophile. It is also observed that the metallic centre is coordinated to the two phosphorus atoms of the catalysts and to the oxygen and nitrogen atoms of the azomethine ylide. This coordination

pattern leads to the blockage of the *Re* face of (*S*)-**A** by one of the phenyl groups of the phosphine unit (Figure 6). This steric hindrance is also generated by the (*S*)-Binap moiety, in which the two α-naphthyl subunits form a dihedral angle of ca. 75 deg.

<Figure 6>

<Scheme 13>

The low enantioselection in the case of acrylates, was a serious drawback because this is the key step to prepare anti HCV agents. Taking in account the rejection of perchlorate salts by the industry and the poor coordination of this anion to the metal centre, we decide to change to another anion which was weakly bonded to the central metal. According to this experience, we envisaged that the poorly coordinating anion SbF_6^- would modify the chiral domain of the metal complex vacancy, thus allowing the reaction with acrylates [37].

The standard reaction shown in Scheme 10, between methyl benzylideneiminoglycinate **35** (R^1 = H, R^2 = Me, R^3 = Ph) and NMM, was employed for the small optimization tests. Initially, the reaction conditions were identical to those previously described for Binap-$AgClO_4$ catalyzed

1,3-DC, that means, 5 mol% of the catalyst (formed with equimolar amounts of chiral Binap and $AgSbF_6$), in toluene at room temperature for 16 h, in the presence of Et_3N as base. Both of the $AgClO_4$ and $AgSbF_6$ catalyzed reactions gave identical results of the cycloadduct *endo*-**46** (R^1 = H, R^2 = Me, R^3 = Ph) (90% yield, >98:2 *endo*:*exo* ratio, and >99% *ee*).

The reaction was also carried out with the isolated complex formed by the addition of equimolar amounts (*S*)-Binap **44** and $AgSbF_6$, obtaining almost identical results to those described for the reaction carried out with $AgClO_4$. However this $AgSbF_6$ derived complex became darker upon standing being much more unstable than the identical complex generated with $AgClO_4$. So, the *in situ* generation of the catalytic complex, avoiding the light exposure during the whole process was preferred for all the transformations described in this section.

The presumed catalytic monomeric species in solution are identical to those the reported previously with different anions [36]. In fact, the 1:1 (*R*)- or (*S*)-Binap **44** and $AgSbF_6$ complexes were characterized by ESI-MS experiments and ^{31}P NMR. ESI-MS reveled a M^++1 signal at 731 corresponding to the monomeric 1:1 Binap-Ag^I complex and a tiny one at 1353 corresponding to the 2:1 Binap:$AgSbF_6$. ^{31}P NMR ($CDCl_3$) of 1:1 (*R*)- or (*S*)-Binap and $AgSbF_6$ (10% aqueous polyphosphoric acid as internal reference) afforded signals at 15.31 ppm (d, $J_{P\text{-}Ag(109)}$ = 242 Hz)

(15.26 ppm for Binap-$AgClO_4$ complex) and 15.45 ppm (d, $J_{P\text{-}Ag(107)}$ = 242 Hz) (15.35 ppm for Binap-$AgClO_4$ complex). The absence of NLE is another data supporting the existence of a monomeric species in the enantioselective catalytic process in solution.

In general we could observe that isolated chemical yields of compounds **46** were identical to each other finding a higher enantioselection in those reactions promoted by the complex formed by (*S*)-Binap and $AgSbF_6$, specially when the aromatic moiety was substituted at different positions or not (Table 5, entries 1-6). Whilst the reaction with NEM do not represent any difference with respect to those results obtained in the (*S*)-Binap-$AgClO_4$ (Table 5, entry 7), the reaction carried out with *N*-phenylmaleimide (NPM) was much more enantioselective in the presence of (*S*)-Binap-$AgSbF_6$ complex (82% *ee*, *vs* 62% *ee* obtained with perchlorate derived chiral complex) and >98:2 *endo*:*exo* ratio was obtained (Table 5, entry 8). Computational calculations revealed the existence of stereoelectronic effects between the phenyl group of the NPM and the Binap-$AgClO_4$ catalyst. However, in the case of Binap-$AgSbF_6$ catalyzed process seemed that the less coordinating anion decreased the steric congestion of the transition state.

The incorporation of a bulky substituent at the α-position of the 1,3-dipole precursor as occurred in the methyl benzylideneimino-

phenylalaninate **35** (R^1 = Ph, R^2 = Me, R^3 = Ph, R^4 = Me) was successfully overcome using the standard reaction conditions. Here, the *endo*-adduct **46** (R^1 = Ph, R^2 = Me, R^3 = Ph, R^4 = Me) was obtained as single enantiomer (99% *ee*) in very good chemical isolated yield (86%). Clearly, this reaction promoted by (*S*)-Binap-$AgSbF_6$ complex improved the results obtained in the reaction performed with the perchlorate salt.

<Scheme 14>

<Table 5>

Acrylates, maleates, and fumarates were not suitable dipolarophiles neither for the (*S*)-Binap **44**-$AgSbF_6$ (<30% *ee* and <40% *ee*, respectively) nor for (*S*)-Binap **44**-$AgClO_4$ catalysed processes such as it has been described (see above). However *trans*-1,2-bis(phenylsulfonyl)ethylene **57** afforded very interesting results of *endo*-cycloadducts **58** (Scheme 15). This electrophilic alkene is a synthetic equivalent of acetylene and allows some useful synthetic transformations [25f]. The reaction operates under the standard conditions but taking 48 h to complete. This 1,3-DC, not evaluated previously with the chiral perchlorate complex, was performed using both silver salts (Table 6). The four methyl iminoglycinates **35** tested

in this reaction under the control of (*S*)-Binap-$AgSbF_6$ catalytic complex afforded *endo*-cycloadducts **58** in good chemical yields (80-91%) and very high enantioselectivities (88-92% *ee*) (Table 6). The enantioselection was higher than the analogous exhibited by the chiral silver complex in all of the entries described in Table 6, especially in the reaction of *p*-tolyliminoester, 88% *ee vs* 28% *ee*, (Table 6, entry 3). This is the first synthesis of the disulfonyl *endo*-**58** cycloadducts, whose absolute configuration was determined by NOESY experiments, and indirectly by comparison of the corresponding HPLC analysis with those described in the literature for the *exo*-cycloadducts [25f].

<Scheme 15>

<Table 6>

The multicomponent version of this transformation was attempted using the best result depicted in Tables 5 and 6. Thus, benzaldehyde/NMM or 3-pyridinecarbaldehyde/disulfone **57**, glycine methyl ester hydrochloride, triethylamine (1.05 equiv), (*S*)-Binap-$AgSbF_6$ (5 mol%), were put together in toluene and the resulting mixture was allowed to react at rt for 48 h. The results obtained for compound *endo*-**46** (R^1 = H, R^2 =

Me, R^3 = Ph, R^4 = Me) or *endo*-**58** (Ar = 3-pyridyl) were impressive (88% yield, >99% *ee*, or 86% yield, 98% *ee*, respectively, Scheme 16), taking in account that the analogous reactions in the presence of (*S*)-Binap-$AgClO_4$ complex failed. Although very activated aminomalonates have been involved as one of the three components of the enantioselective organocatalyzed 1,3-DC [29d,l,m,n], this is the first occasion that a three-component transformation is enantioselectively performed in the presence of a chiral Lewis acid [37].

<Scheme 16>

Evaluating all of these results, it was demonstrated how important resulted to be the anion in this sensitive enantioselective process, which is controlled by many parameters. But the main conclusion extracted was the impossibility to design efficiently the key step for the synthesis of antiviral agents employing a combination between chiral Binap **44** ligand and a silver(I) salt. Based on the semiempirical calculations described, and the two images of the Figure 6, it looks like there is not enough space in the enantiodiscrimination domain for the accommodation neither of bulky substituents of the nitrogen atom in maleimides nor ester groups of the acrylate moiety. The Csp^2 of the ester carbonyl group were not so good

coordinating atom as a nitrogen atom or as oxygen atom belonging to a sulfoxide or a sulfone did. In this last case, the disulfone is much more reactive due to the lower energy of its LUMO. So, it is reasonable think in a chiral-Binap **44**-gold(I) complex, as a larger metal cation, able to maintain both of the same properties of the silver(I) complexes and the coordination with all these components in an efficient manner.

Toste *et al.* published the first quiral gold 1,3-dipolar cycloaddition between mesoionic azomethine ylides (münchnones) with electron-poor alkenes catalyzed by Cy-Segphos$(AuCl)_2$. The reaction afforded in all cases only the *exo*-adduct in high yields and very good enantioselections [26e]. However, the classical 1,3-dipolar cycloaddition of iminoesters and electrophilic olefins catalyzed by gold complexes was not studied previously [38].

The gold(I) cation has only two coordination sites and its linear geometry makes asymmetric catalysis extremely difficult. Fortunately, a key to the development of enantioselecive gold(I)-catalyzed transformations have been the identification of enantiomerically pure bis(gold)-chiral diphosphine complexes of the form $[(AuX)_2(P\text{-}P)^*]$ as catalysts for enantioselective transformations. A clear and recent example of the isolation, identification, and characterization of two chiral Binap-gold(I) complexes **59** and **60** (Chart 11) has been reported by Puddephatt *et*

al [39]. These complexes were prepared by mixing (Me_2S)AuCl and the corresponding amount of the chiral Binap ligand. The resulting gold chloride complexes were treated with different silver salts for 1 h in toluene and the suspension was filtered through a celite plug. The remaining solution was evaporated obtaining **59** or **60** in 89 and 96% yields, respectively (Chart 11).

<Chart 11>

These cationic complexes were immediately employed without any other purification in the catalytic enantioselective 1,3-DC of the imino ester **35** (R^1 = H, R^2 = Me, R^3 = Ph) and NMM in toluene at rt. The cleanest reaction mixtures and highest conversions were obtained with complexes bearing trifuoroactate as counteranion. When this cycloaddition was performed in the presence of 10 mol% of diisopropylethylamine (DIPEA) and **59**, product *endo*-**46** (R^1 = H, R^2 = Me, R^3 = Ph) was obtained with high conversion but in racemic form. However, dimeric complexes type **60** resulted to be more appropriate. In the case of the chiral complex **60** 74% *ee* of compound *endo*-**46** (R^1 = H, R^2 = Me, R^3 = Ph) was obtained in the presence of DIPEA, whereas without base, a 99% *ee* was obtained. The attempt to reduce the catalyst loading to a 5 mol% was not successful such

as reveals the lower enantioselection (60% *ee*) obtained. In every example the major cycloadduct obtained was the *endo* (>98:2 *dr*) according to the NMR experiments of the crude products. The absolute configuration of proline derivatives **46** was confirmed by comparison of their chiral HPLC retention times and specific optical rotations with those described for enantiomerically pure samples.

<Scheme 17>

The scope of this chiral gold(I)-catalyzed enantioselective 1,3-DC was studied using different iminoesters **35** and maleimides under the best reaction conditions described before (Scheme 17). In the Table 7 a comparison between the results obtained with chiral gold(I) complex **60** and chiral Binap-AgOTf complex was made. In the first examples it was included the reactions of NMM with iminoester **35** (R^1 = H, R^2 = Me, R^3 = Ph) where the absence of base was crucial for the achievement of a good enantioselection (Scheme 18, and Table 7, entries 1 and 2). In the case of employing NEM and NPM, in the absence of base, products **46** (R^1 = H, R^2 = Me, R^3 = Ph, R^4 = Et, Ph) were obtained with higher enantioselectivity than when the reaction was catalyzed by the chiral silver complex (Table 7, entries 3, and 5). However, in the presence of DIPEA (10 mol%) the chiral

silver(I) catalyzed process is more efficient except in the reaction done with NPM (Table 7, compare entries 4, and 6). In fact, the result obtained when NPM was employed as a dipolarophile (Table 7, entry 5) is particularly noteworthy because it is the best *ee* (80% *ee*) achieved till date with chiral Binap and chiral phosphoramidite ligands. When (S_a)-Binap-AgTFA was used as catalyst, racemic product was obtained. For the 1,3-DC of other arylideneaminoesters **35** (R^1 = H, R^2 = Me, R^3 = Ar), and maleimides the conversions are identical independently of metal cation employed. In the case of 2-naphthyl derived iminoester the enantioselections were very close to each other, but with NPM chiral gold(I) catalysts **2** (X = TFA) (Table 7, entry 7) again was much more efficient generating the highest enantioselections. The dipole precursors **35** containing an *ortho*-substituent in the aryl moiety, were appropriate sterically hindered starters in the gold(I)-catalyzed 1,3-DC with NMM affording *endo* compounds **46** with 99 and 88% *ee*, respectively. In both examples the resulting enantioselections induced with the corresponding chiral silver(I) complex were very poor (Table 7, entries 8 and 9). The *para*-substituted methyl iminoglycinates **35** underwent the gold(I) and the silver(I)- mediated 1,3-DC obtaining identical enantioselections (Table 7, entry 10). The insertion of a substituent at the α-position of the 1,3-dipole precursor was next evaluated. Thus, when methyl

benzylideneiminophenylalaninate **35** (R^1 = Ph, R^2 = Me, R^3 = Ar) was allowed to react with NMM under the standard reaction conditions, the reaction performed with the gold(I) complex needed 24 h more than the corresponding reaction using the analogous silver(I) complex for achieving almost total conversions (Scheme 18). The enantioselection showed by (S_a)-Binap-AuTFA complex (99% *ee*) was higher than in the example using (S_a)-BinapAgTFA (65% *ee*) as catalyst (Table 7, entry 11).

<Scheme 18>

<Table 7>

According to the previous experience obtained from chiral Binap-silver(I) complexes, we also tested the efficiency of the Binap-gold(I) trifluoroacetate complexes in the enantioselective cycloaddition of azomethine ylides and *trans*-1,2-bis(phenylsulfonyl)ethylene **57** (Scheme 19 and Table 8). The reaction, performed with 5 mol % of the gold(I) **60** as catalyst, afforded cycloadducts **58** in a non predictable enantioselectivities in the absence or in the presence of DIPEA (20 mol%) as base. In the case of product **35** (R^3 = Ph), a lower enantiomeric excess was obtained when (S_a)-Binap-AgTFA was used as catalyst (Table 8, compare entries 1 and 2).

Compound *endo*-**58** (R^3 = 2-naphthyl) was obtained in better enantiomeric excesses in the absence of base (compare in Table 8, entries 3 and 4). The rest of the examples gave the best enantioselections in the absence of base and mediated by gold(I) catalyst **60** (Table 8, compare entries 5 and 6, 7 and 8, 9 and 10).

The absolute configuration of the *endo*-cycloadducts was again assigned according to the chiral HPLC retention times and by comparison of the physical properties of the isolated samples with the properties published in the literature for the analogous compounds.

<Scheme 19>

<Table 8>

Chiral (R_a)- and [(S_a)-Binap-AuTFA] complexes **60** work as multifunctional catalysts [40] acting as Lewis acid coordinating the dipole and, presumably, the dipolarophile, and as Brønsted base in the enantioselective 1,3-DC of azomethine ylides and maleimides or disulfone **57**.

When other dipolarophiles such as methyl or *tert*-butyl acrylate, dimethyl maleate, and diisopropyl fumarate were allowed to react with

inimoester **35** (R^1 = H, R^2 = Me, R^3 = Ph), under the optimized reaction conditions, high yields of the corresponding *endo*-cycloadducts were obtained but with very low enantioselections. The results obtained with acrylates were very disappointed. In fact, they are the key transformations for the achievement of the very promising antiviral agents against the virus responsible of the hepatitis C. In spite of this drawback, we decided start the preparation of **7**, the most potent second generation antiviral agent. It possesses a sophisticated structural arrangement, bearing a thiazole ring instead of the phenyl group and an isobutyl residue bonded to the α-position of the iminoester. To our surprise, when the general reaction was performed with iminoglycinate **35** (R^1 = Bu^i, R^2 = Me, R^3 = 2-thiazole) and *tert*-butyl acrylate in the presence of triethylamine (10 mol%) an gold(I) catalyst **60** (5 mol%), the resulting cycloadduct *endo*-**45** (R^1 = Bu^i, R^2 = Me, R^3 = 2-thiazole) was obtained in 79% *ee* (at rt), whilst only a 40% *ee* could be achieved by intermediacy of the chiral catalyst (*S*)-Binap **44**-AgTFA [41].

Previously to our work, GSK laboratories obtained this antiviral agent with moderate enantioselection (74% *ee*). In fact, a further 1,1'-binaphthyl-2,2'-dihydrogen phosphate assisted chiral resolution of **7** was performed in order to obtain pure compound *endo*-**7** with a 99.8% *ee* [29i].

With this second objective almost covered, semiempirical and DFT studies are currently underway, in order to clarify the enantiodescrimination of the catalytic gold(I) complex **60**. We are also searching for the most convenient route for developing the synthesis of potent antiviral agent **9**, which constitutes the third challenge of this specific research area.

Conclusions

For the diastereoselective synthesis of prolines by silver-catalyzed 1,3-DC of stabilized azomethine ylides derived from iminoesters and acrylate, the corresponding lactate derivative exhibited high yields and diastereoselectivities. However, the enantioselective version of these type of processes using chiral silver complexes have shown higher reaction scope affording excellent *endo*-diastereoselection and high enantioselectivity. Monodentate ligands such as chiral phosphoramidites and silver perchlorate catalyzed the enantioselective synthesis of polysubstituted prolines using different dipolarophiles. In the case of chiral Binap and silver perchlorate or silver hexafluoroantimonate only maleimides and bis-1,2-(phenylsulfonyl)ethylene are appropriate dipolarophiles. Nevertheless, recent experiments with binap-gold trifluoroacetate complexes have shown promising results for the general

synthesis of prolines using different type of dipolarophiles and sterically hindered dipole precursors (such as α-substituted iminoesters). These studies were focused to the synthesis of highly active HCV inhibitors, being the Binap-gold complexes the best catalysts. DFT calculations explained the diastereo- and enantioselectivities observed in these processes, offering a reasonable explanation according to the steric interactions in the transition states.

Acknowledgements

This work has been supported by the DGES of the Spanish Ministerio de Ciencia e Innovación (MICINN) (Consolider INGENIO 2010 CSD2007-00006, FEDER-CTQ2007-62771/BQU, and by the Hispano-Brazilian project PHB2008-0037-PC), Generalitat Valenciana (PROMETEO/ 2009/039), and by the University of Alicante (GITE-09020-UA). We also thank all the participants of this cycloaddition project: M. G. Retamosa, M. Martín-Rodríguez, A. de Cózar, F. P. Cossío, E. Crizanto de Lima, P. R. R. Costa, A. G. Dias and F. L. Wu.

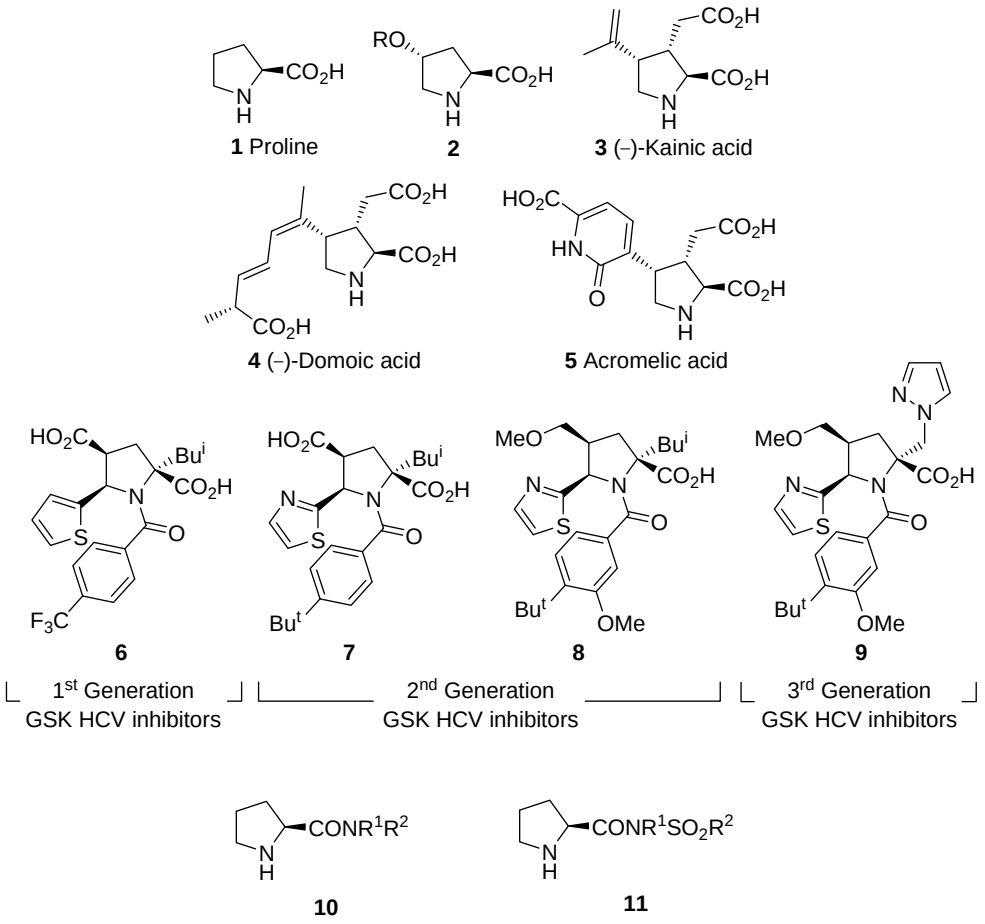

Chart 1. Useful proline derivatives.

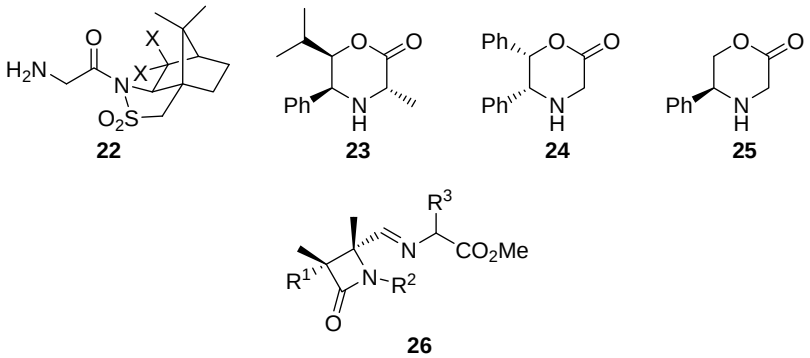

Chart 2. Some recent chiral 1,3-dipole precursors.

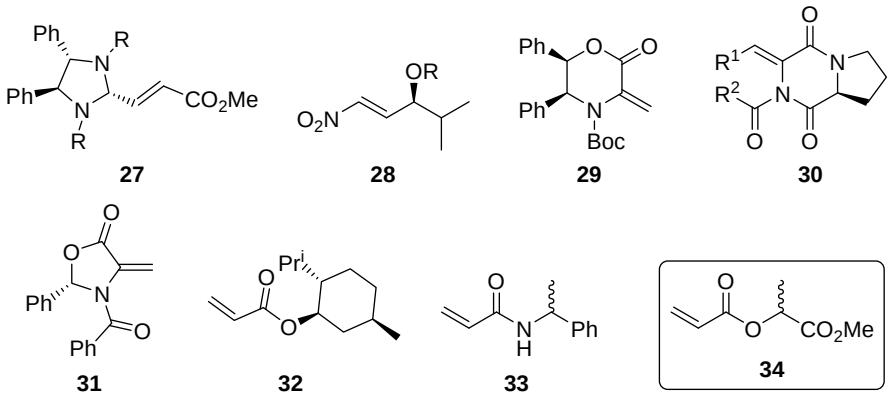

Chart 3. Some recent chiral dipolarophiles.

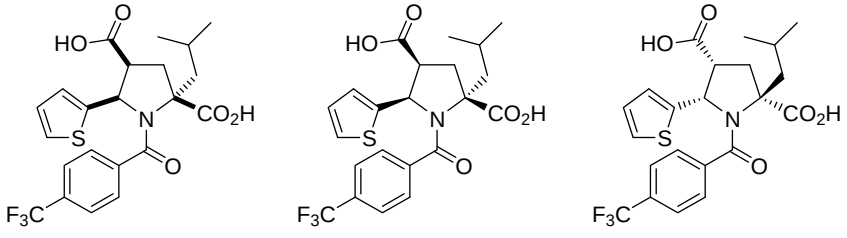

Chart 4. Biological activity of the most active 1st GSK generation of HCV inhibitors.

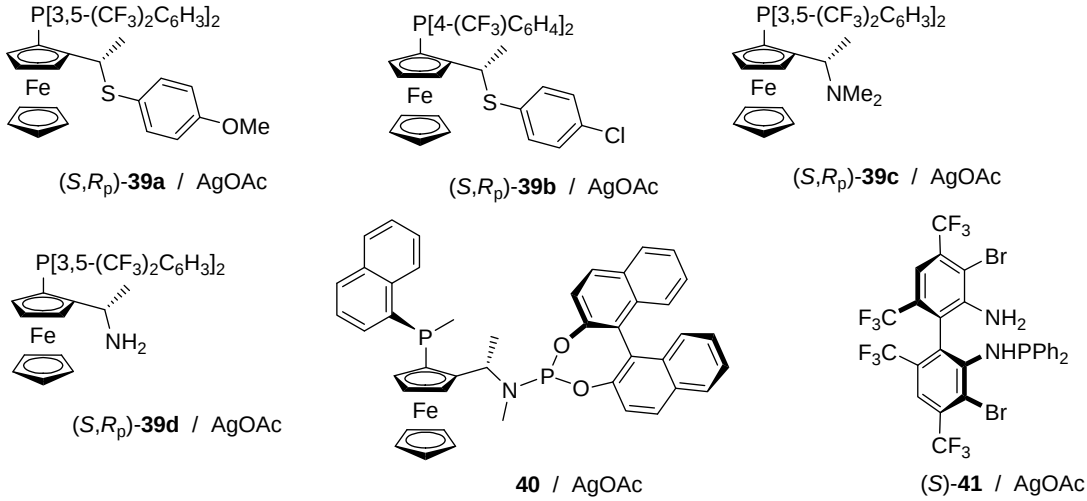

Chart 5. Chiral ligands / silver salts used to generate chiral Lewis acids employed in the enantioselective 1,3-DC of azomethine ylides and dipolarophiles.

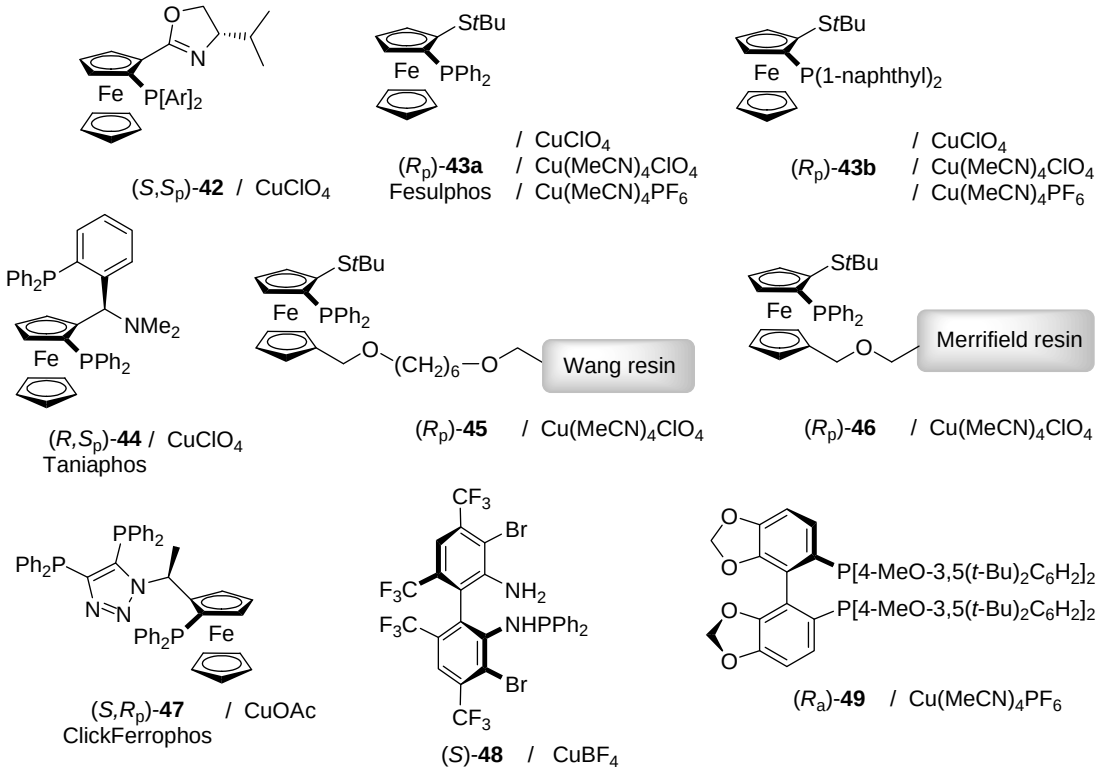

Chart 6. Chiral ligands / copper(I) salts used to generate chiral Lewis acids employed in 1,3-DC of azomethine ylides and dipolarophiles.

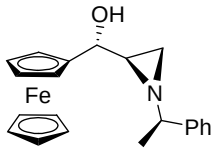

50 / $Zn(OTf)_2$

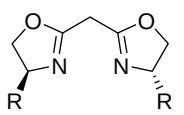

51a, R = Ph / $Ca(OiPr)_2$
51b, R = *i*Pr / $Ca(OiPr)_2$

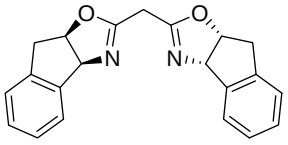

52 / $Ca(OiPr)_2$

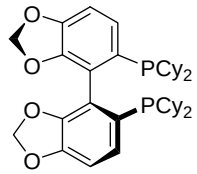

(S_a)-Cy-Segphos **53** / $(AuOBz)_2$

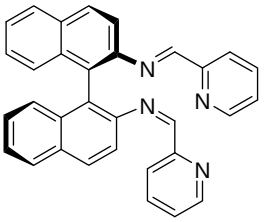

(R_a)-**54** / $Ni(ClO_4)_2 \cdot 6H_2O$

1

2 **Chart 7.** Chiral ligands / zinc(II), calcium(II), gold(I), or nickel(II) salts
3 used to generate chiral Lewis acids employed in 1,3-DC of azomethine
4 ylides and dipolarophiles.

5

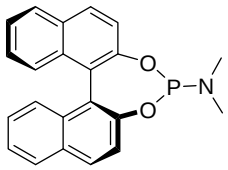

(*S*)-Monophos **42**

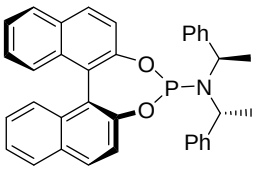

(S_a,*R*,*R*)-**43**

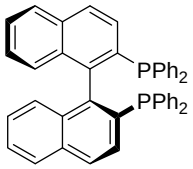

(*S*)-Binap **44**

6

7 **Chart 8.** Chiral ligands employed by Najera's group.

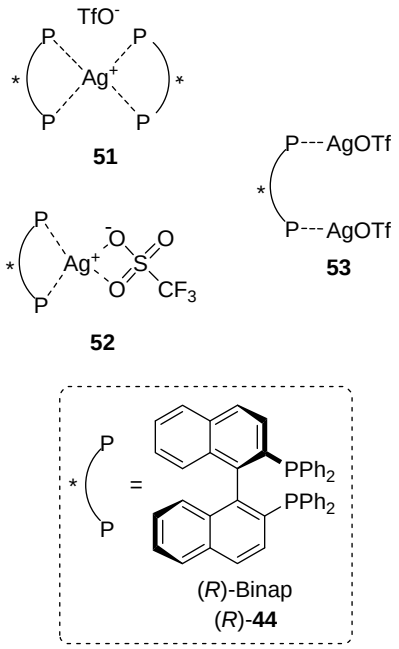

Chart 9. Identified Binap-AgOTf species.

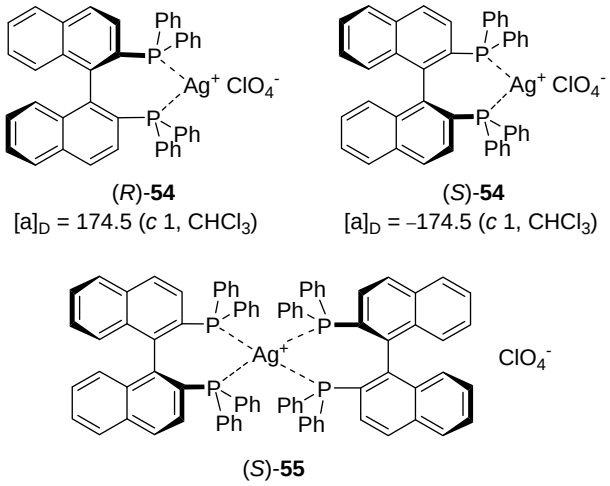

Chart 10. Chiral Binap-silver complexes employed.

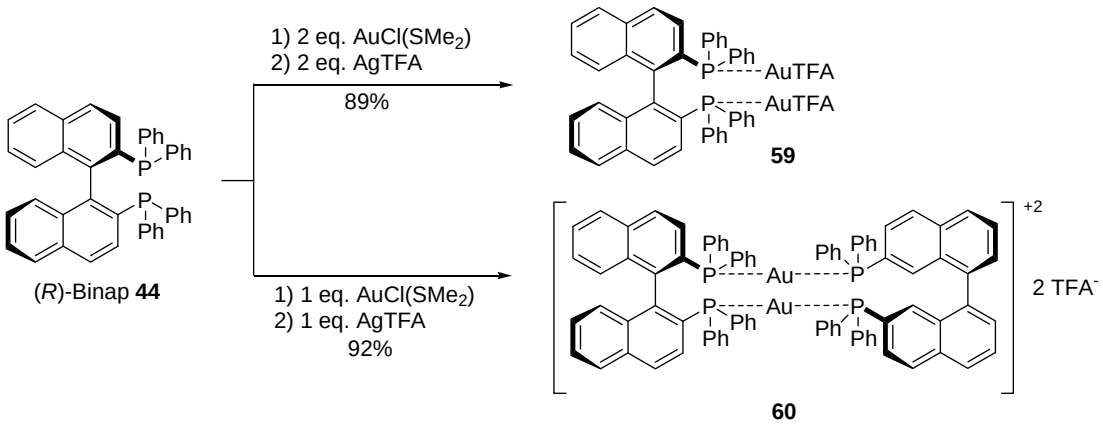

Chart 11. Chiral Binap-gold complexes employed.

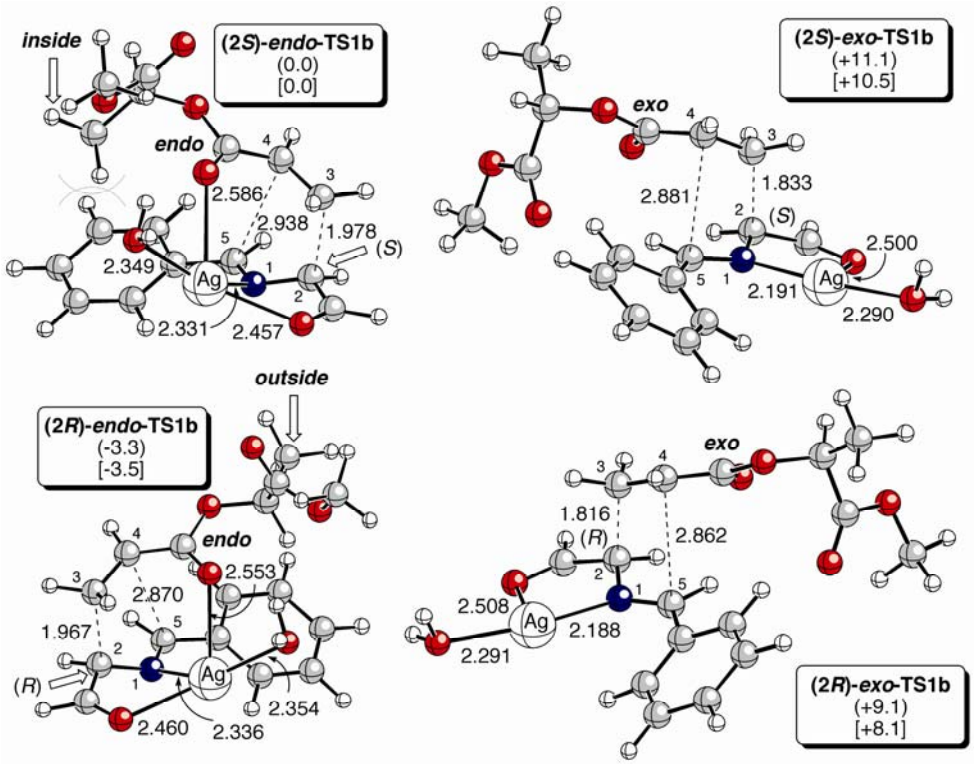

Figure 1. Relative energies of the four possible transition states for the explanation of the observed stereoreoselection.

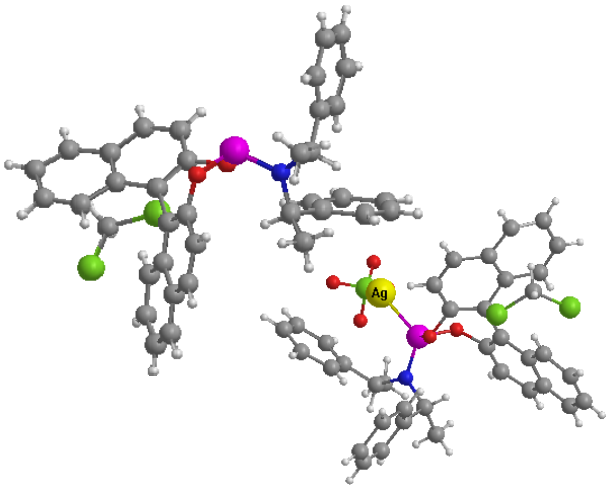

a)

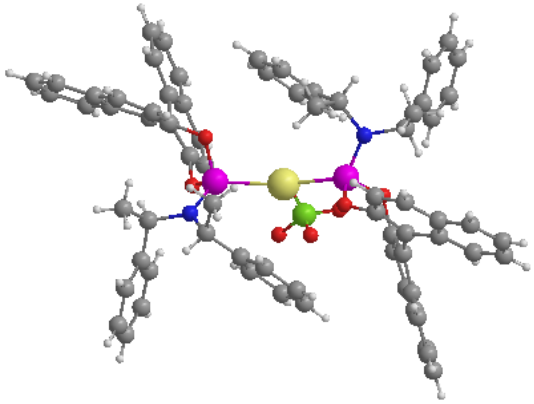

b)

Figure 2. X-Ray diffraction analysis of a) 1:1 **43**-$AgClO_4$ complex and b) 2:1 **43**-$AgClO_4$ complex.

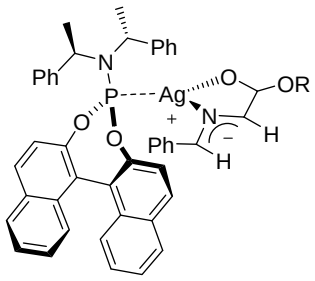

I

Figure 3. Suggested structure of intermediate complex **I**.

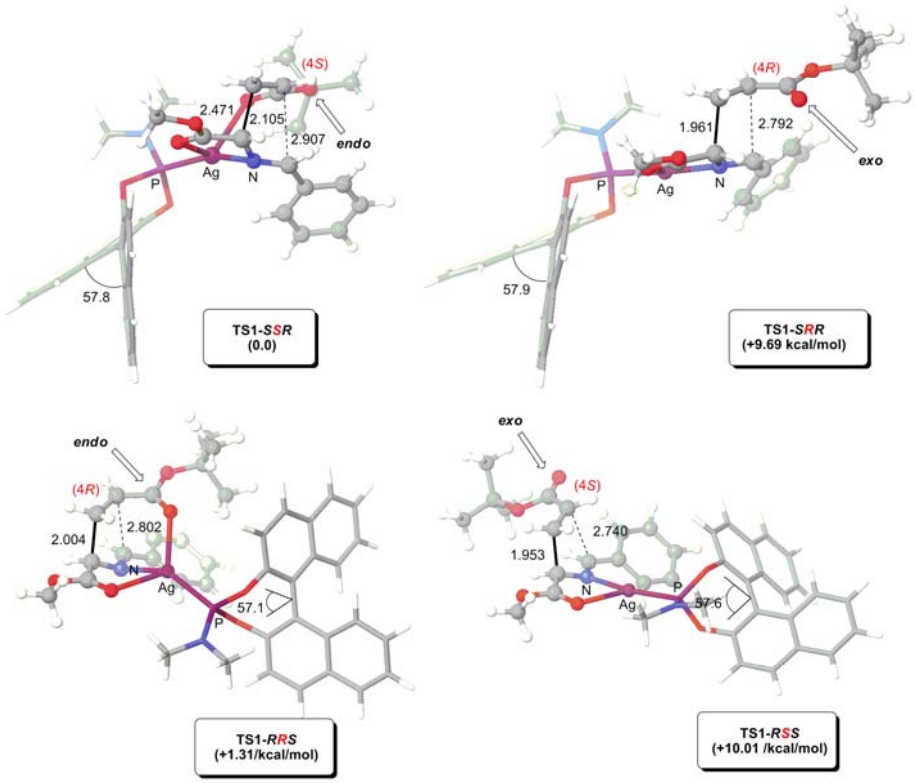

Figure 4. Chief geometric features saddle relative energies (in kcal/mol) of the four transition structures associated with the first step in the reaction between *tert*-butyl acrylate and complex formed by (S_a)-Monophos **42** and imine **35**.

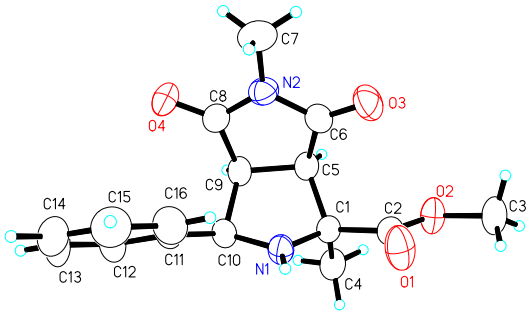

Figure 5. ORTEP of cycloadduct (2*R*,3*S*,4*S*,5*S*) *endo*-**46** (R^1 = Me, R^2 = Me, R^3 = Ph, R^4 = Me).

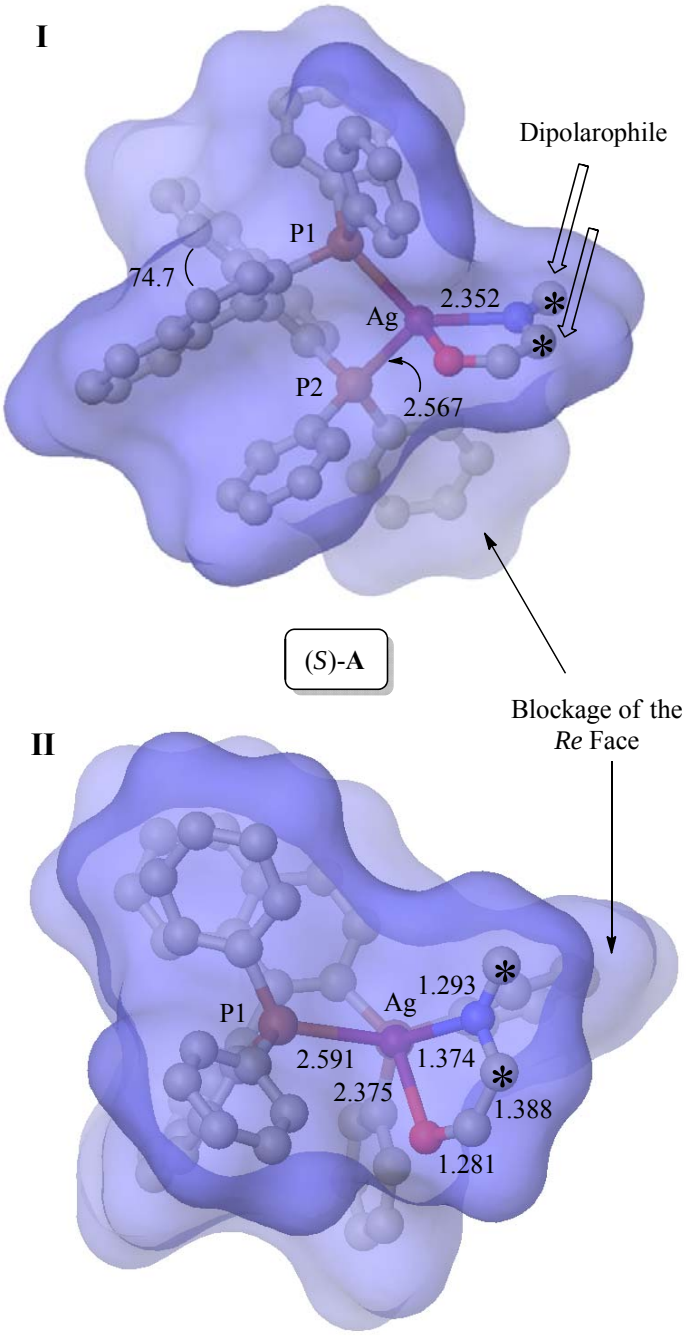

Figure 6. I: Fully optimized structure (B3LYP/LANL2DZ&6-31G* level) of (*S*)-**A**. The hydrogen atoms have been omitted for clarity. The carbon

atoms of the azomethine ylide moiety have been highlighted with asterisks. Bond distances and dihedrals are given in Å and deg., respectively. The molecular surface (Probe radius: 1.4 Å) is also included. II: View over the *Si* face of (*S*)-**A** along the axis determined by the Ag and P2 atoms.

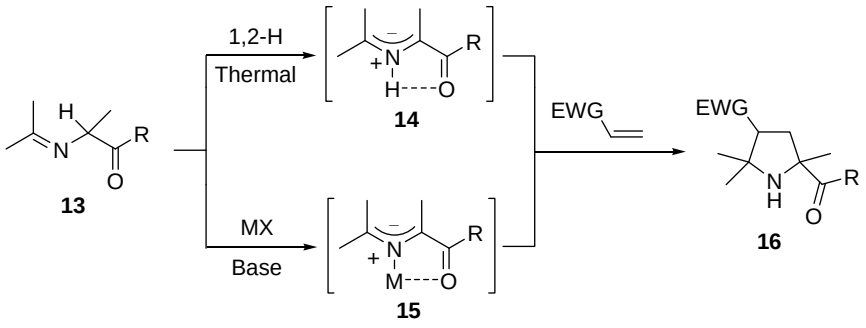

Scheme 1

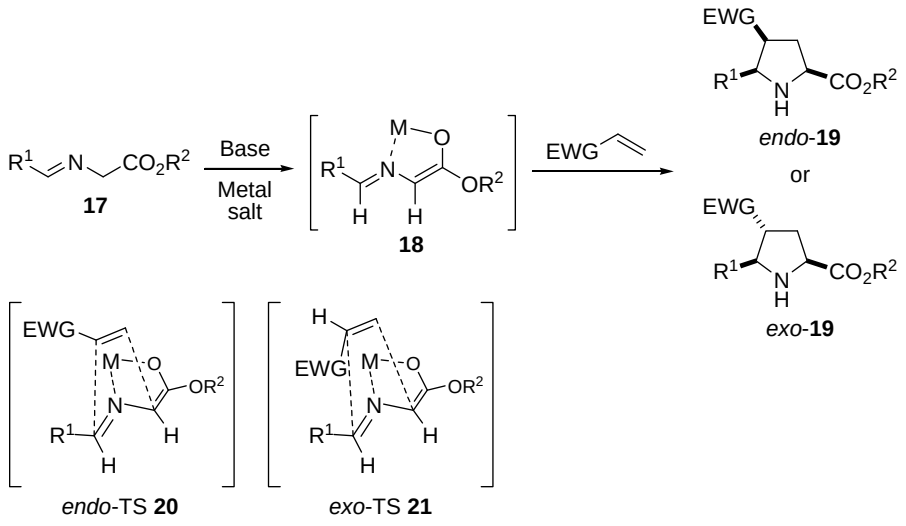

Scheme 2

1

2 **Scheme 3**

3

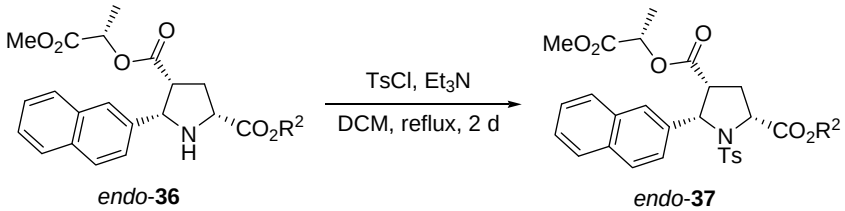

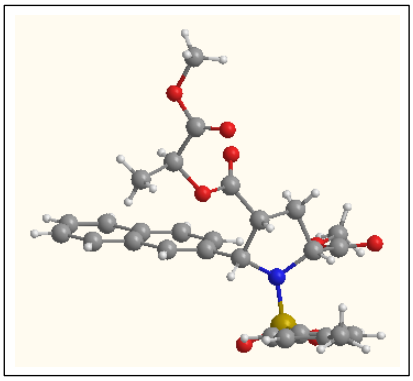

4

5 **Scheme 4**

6

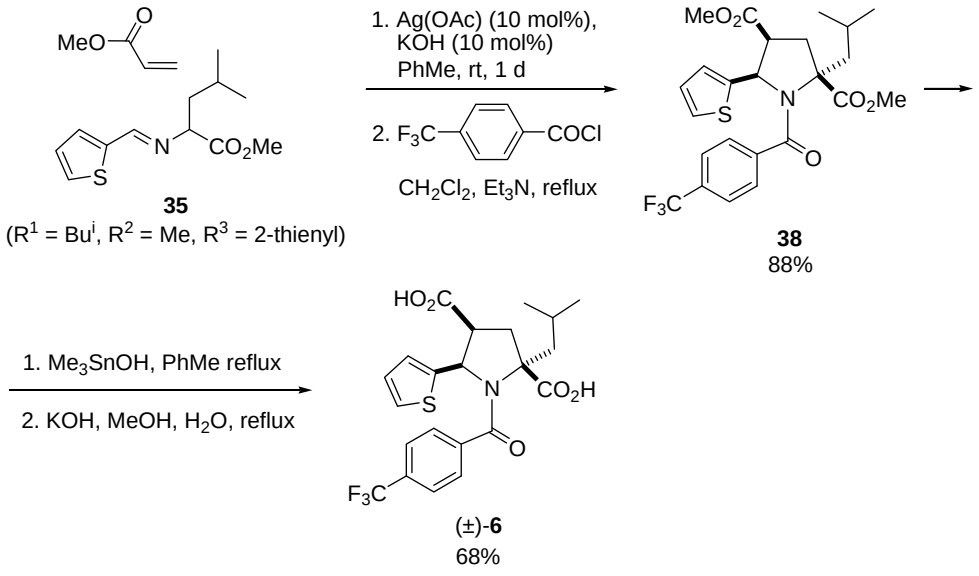

1

2 **Scheme 5**

3

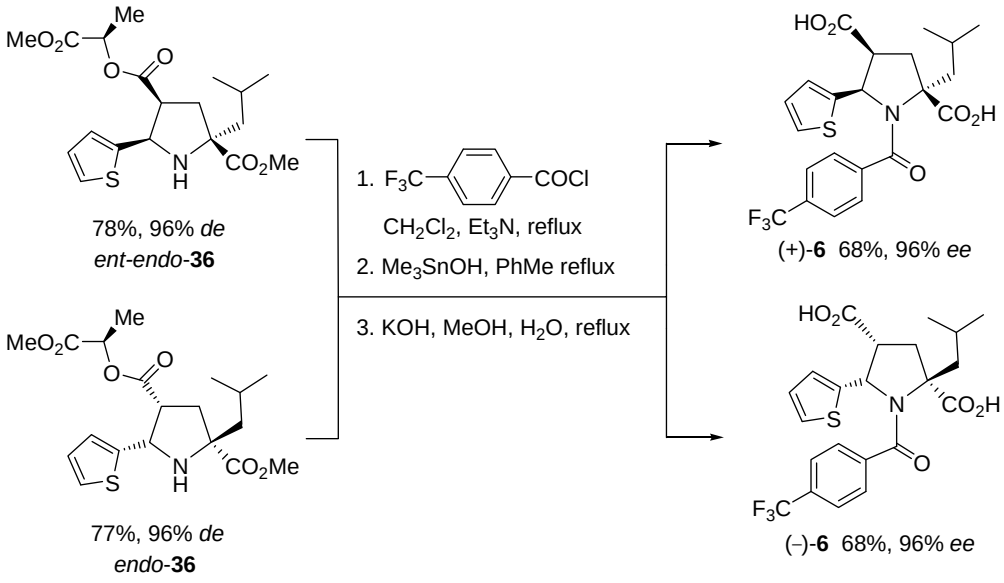

4

5 **Scheme 6**

6

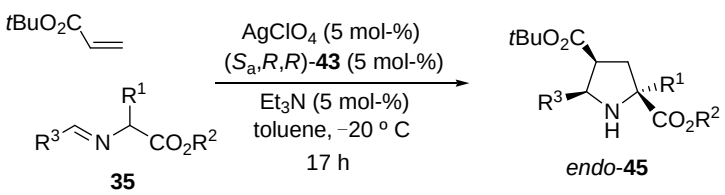

7

1 **Scheme 7**

2

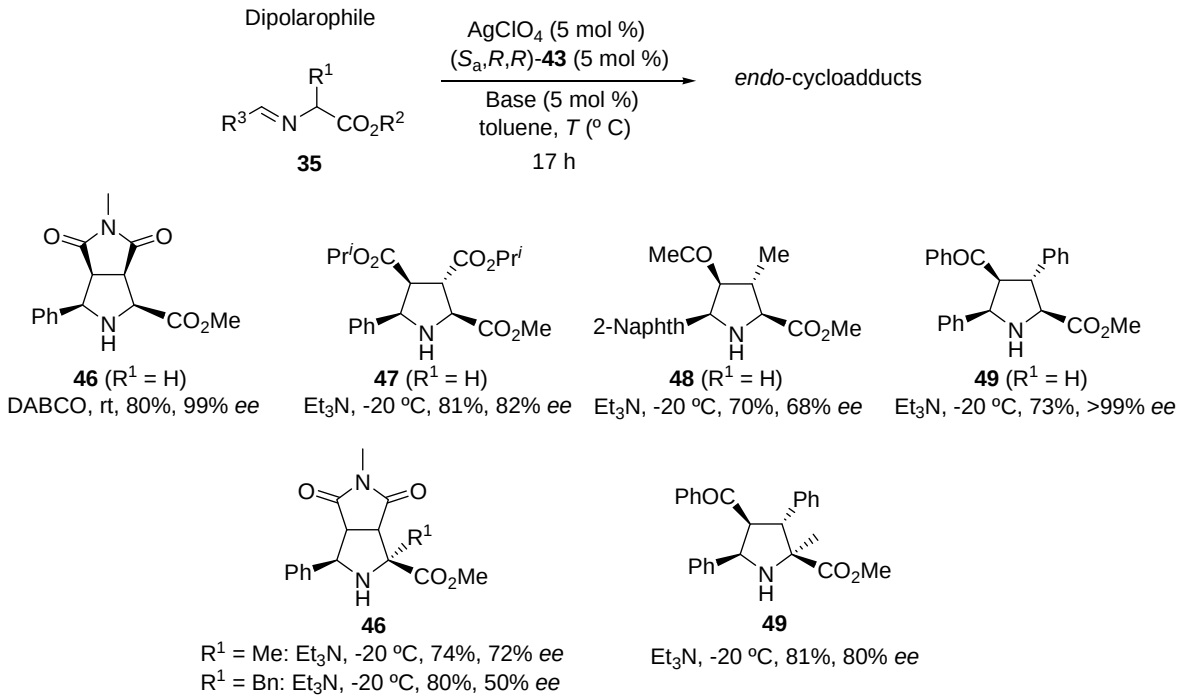

3

4 **Scheme 8**

5

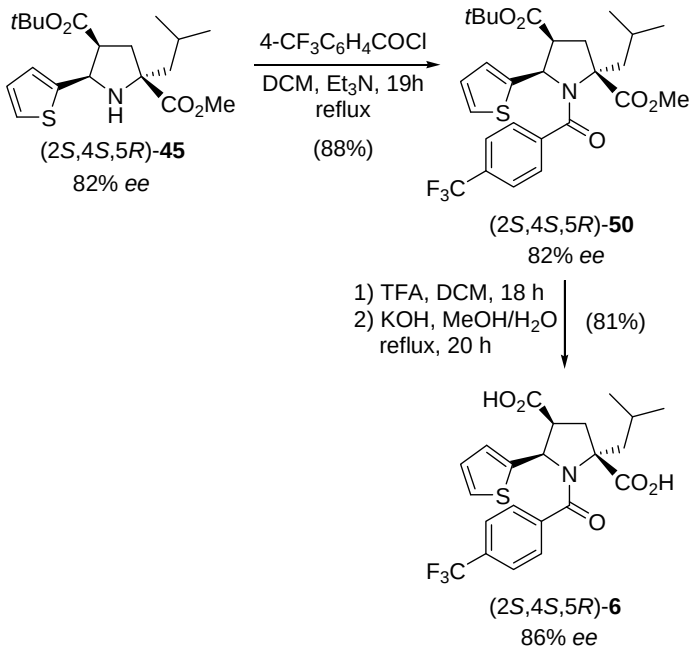

6

7 **Scheme 9**

1

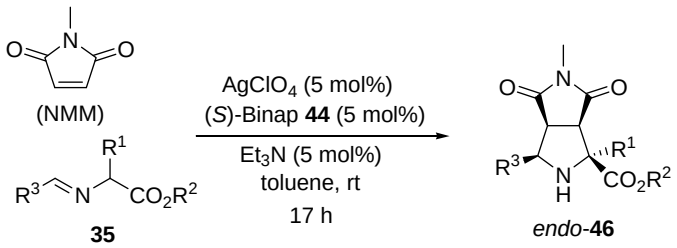

2

3 **Scheme 10**

4

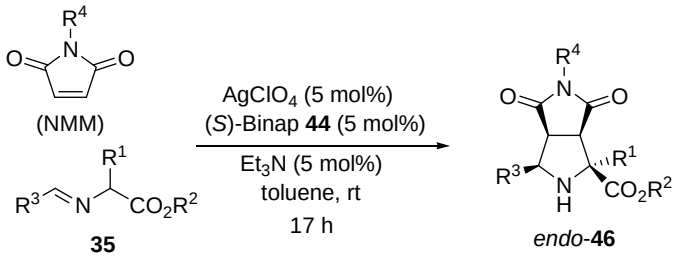

5

6 **Scheme 11**

7

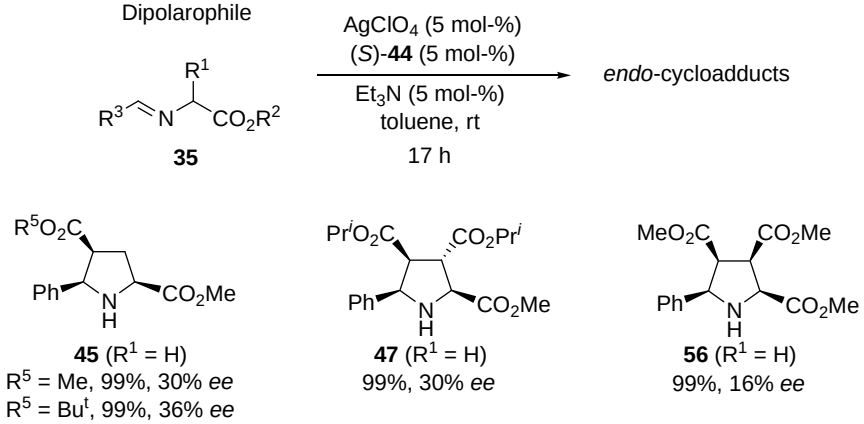

8

9 **Scheme 12**

10

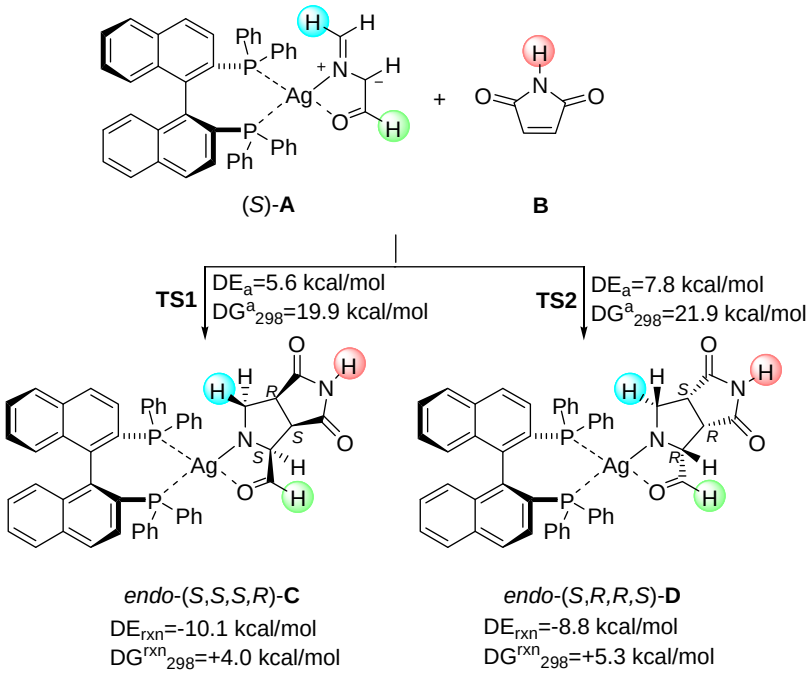

Scheme 13. Model reaction used in the computational studies.

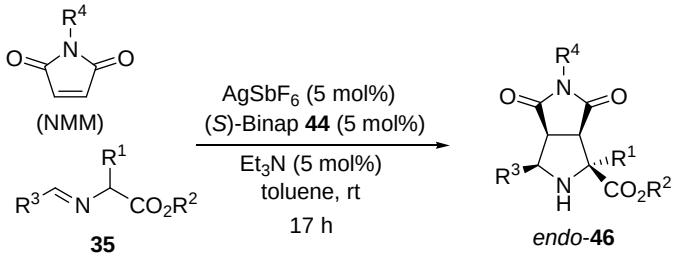

Scheme 14

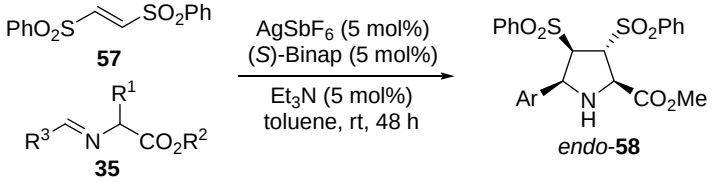

Scheme 15

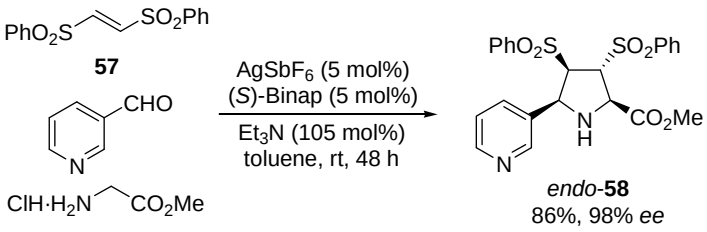

1

2

3 **Scheme 16**

4

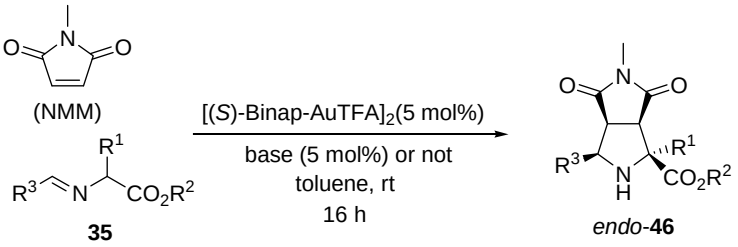

5

6 **Scheme 17**

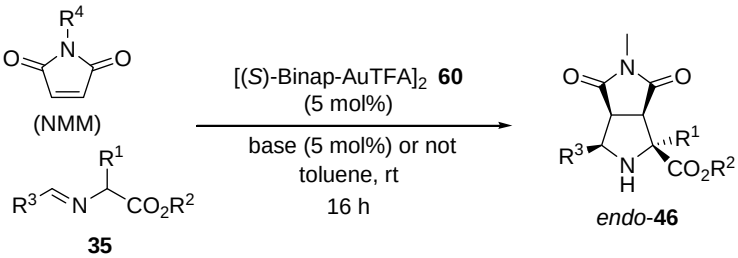

7

8 **Scheme 18**

9

10

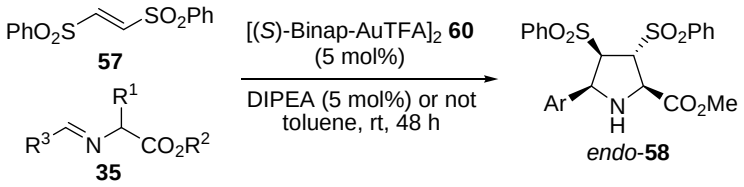

Scheme 19

Table 1 1,3-DC between chiral acrylate (*S*)-**34** and iminoesters **35**.

Entry	R^1	R^2	R^3	Yield (%)[a]	*de* (%)[b]
1	H	Me	Ph	64	94
2	H	Pr^i	Ph	63	92
3	H	Bu^t	Ph	73	99
4	H	Me	2-Naphthyl	60	90
5	H	Bu^t	2-Naphthyl	70	99
6	Me	Me	Ph	65	90
7	Me	Bu^t	Ph	70	92
8	Bn	Me	2-Naphthyl	65	84
9	Bn	Me	2-Thienyl	65	95
10	Bu^i	Me	2-Thienyl	77	96
11	Bu^i	Pr^i	2-Thienyl	82	82
12	Bu^i	Bu^t	2-Thienyl	83	87

[a] Isolated yield after purification by flash chromatography. [b] Determined by chiral HPLC.

Table 2 Enantioselective 1,3-DC of iminoesters **35** (R^2 = Me) promoted by 1:1 $AgClO_4$:(S_a,*R*,*R*)-**43** catalytic complex.

Entry	R^1	R^2	R^3	Yield (%)[a]	*ee* (%)[b]
1	H	Me	Ph	80	88
2	H	Pr^i	Ph	83	99
3[c]	H	Me	2-ClC_6H_4	80	99
4	H	Me	2-Naphthyl	84	91
5	H	Pr^i	4-$MeOC_6H_4$	80	98
6	H	Pr^i	4-ClC_6H_4	77	94
7	Me	Me	Ph	78	94
8	Bn	Me	Ph	77	98
9	Me	Me	2-Thienyl	70	88
10	Bu^i	Me	2-Thienyl	77	82

[a] Isolated yield after purification by flash chromatography. [b] Determined by chiral HPLC. [c] Reaction performed with DABCO instead of Et_3N.

Table 3 Recycling experiments of 1:1 [(*S*)-Binap **44**]:$AgClO_4$ complex.

Cycle	Reaction (mmol)	**35** mmol[a]	Recovered catalyst (%)	**46** Yield (%)[b]	**46** *ee* (%)[c]
1	1	0.100	95	91	>99
2	1	0.095[d]	93	89	>99
3	1	0.088[d]	92	91	>99
4	1	0.081[d]	90	90	99
5	1	0.073[d]	90	88	98

[a] Recovered after filtration of the crude reaction suspension and washed several times with toluene. [b] Isolated yield of compound *endo*-**46** after recrystallization. The conversions were >99% and the *endo*:*exo* ratio were >98:2 in all of the essayed cycles. [c] Determined by chiral HPLC (Daicel Chiralpak AS). [d] Amount recovered from the previous cycle.

Table 4 Enantioselective 1,3-DC of iminoesters **35** (R^2 = Me) promoted by 1:1 $AgClO_4$:(*S*)-Binap **44** catalytic complex.

Entry	R^1	R^2	R^3	R^4	Yield (%)[a]	*ee* (%)[b]
1	H	Me	Ph	Me	90	>99
2	H	Et	Ph	Me	78[c]	91
3	H	Pr^i	Ph	Me	80[c]	72
4	H	Bu^t	Ph	Me	81[c]	92

5	H	Me	2-Naphthyl	Me	89	>99
6	H	Me	2-ClC_6H_4	Me	82	85
7	H	Me	4-$MeOC_6H_4$	Me	85	99
8	H	Me	2-Thienyl	Me	87	92
9	H	Me	Ph	Et	91	>99
10	H	Me	Ph	Ph	86[c]	62
11	Me	Me	Ph	Me	80	72
12	Bn	Me	Ph	Me	83	64
13	Bu[i]	Me	2-Thienyl	Me	81	74

[a] Isolated yield after purification by flash chromatography. [b] Determined by chiral HPLC. [c] Around a 90:20-85:25 *endo:exo* ratios were observed.

Table 5 Enantioselective 1,3-DC of iminoesters **35** (R^2 = Me) promoted by 1:1 $AgSbF_6$:(*S*)-Binap **44** catalytic complex.

Entry	R^1	R^2	R^3	R^4	Yield (%)[a,b,c]	*ee* (%)[c,d]
1	H	Me	Ph	Me	90 (90)	>99 (>99)
2	H	Me	Ph[e]	Me	90 (90)	>99 (>99)
3	H	Me	2-MeC_6H_4	Me	85 (85)	99 (70)
4	H	Me	2-ClC_6H_4	Me	82 (82)	>99[f] (85)[f]

5	H	Me	4-MeC_6H_4	Me	85 (88)	99 (88)
6	H	Me	4-$MeOC_6H_4$	Me	85 (85)	99 (80)
7	H	Me	Ph	Et	84 (91)	99 (99)
8	H	Me	Ph	Ph	86 (86)	82 (62)[g]
9	Ph	Me	Ph	Me	86 (92)	99 (64)

[a] The *endo:exo* ratio was always >98:2 (^{1}H NMR spectroscopy, and chiral HPLC). [b] Isolated after flash chromatography. [c] In brackets the result obtained previously with (*S*)-Binap-$AgClO_4$ complex. [d] Determined by chiral HPLC of the crude product. Identical *ee* was determined after purification. [e] Reaction performed with (*R*)-Binap-$AgSbF_6$. [f] Reaction performed at ~ 20 ºC. [g] The *endo*:*exo* ratio was approximately 90:10.

Table 6 Enantioselective 1,3-DC of iminoesters **35** (R^2 = Me) and disulfone **57**.

Entry	R^1	R^2	R^3	Yield (%)[a,b,c]	*ee* (%)[c,d]
1	H	Me	Ph	81 (80)	90 (88)
2	H	Me	Ph[e]	90 (90)	90 (88)
3	H	Me	4-MeC_6H_4	91[f] (85)	88 (28)
4	H	Me	3-Pyridyl	83 (82)	93 (78)

5	H	Me	2-Naphthyl	91[f] (88)	92 (80)	

[a] The *endo:exo* ratio was >98:2 (^{1}H NMR spectroscopy, and chiral HPLC). [b] Isolated after column chromatography. [c] In brackets the result obtained with (*S*)-Binap-$AgClO_4$ complex. [d] Determined by chiral HPLC of the crude product. Identical *ee* was determined after purification of **58**. [e] Reaction performed with (*R*)-Binap-$AgSbF_6$. [f] Pure crude yields.

Table 7 Enantioselective 1,3-DC of iminoesters **35** (R^2 = Me) and maleimides promoted by dimeric catalytic gold(I)-complex **60**.

Entry	R^1	R^2	R^3	R^4	Base	Yield (%)[a,b,c]	*ee* (%)[c,d]
1	H	Me	Ph	Me	—	90 (90)	99 (99)
2	H	Me	Ph[e]	Me	—	90 (90)	99 (99)
3	H	Me	Ph	Et	—	99 (99)	99 (99)
4	H	Me	Ph	Et	DIPEA	80 (81)	70 (99)
5	H	Me	Ph	Ph	—	81 (81)	80 (*rac*)
6	H	Me	Ph	Ph	DIPEA	89 (89)	64 (*rac*)
7	H	Me	2-Naphthyl	Ph	—	82 (86)	99 (45)
8	H	Me	2-MeC_6H_4	Me	—	90 (86)	99 (50)
9	H	Me	2-ClC_6H_4	Me	—	80 (80)	88 (60)
10	H	Me	4-$(MeO)C_6H_4$	Me	—	88 (88)	99 (99)

11	Ph	Me	Ph	Me	—	78 (95)	99 (65)

[a] The *endo:exo* ratio was always >98:2 (^{1}H NMR spectroscopy, and chiral HPLC). [b] Isolated after flash chromatography. [c] In brackets the result obtained previously with (*S*)-Binap-AgTFA complex. [d] Determined by chiral HPLC of the crude product. Identical *ee* was determined after purification. [e] Reaction performed with (*R*)-Binap.

Table 8 Enantioselective 1,3-DC of iminoesters **35** (R^2 = Me) and disulfone **57** promoted by dimeric catalytic gold(I)-complex **60**.

Entry	R^1	R^2	R^3	Base	Yield (%)[a,b,c]	*ee* (%)[c,d]
1	H	Me	Ph	DIPEA	81	80 (86)
2	H	Me	Ph	—	74	99 (96)
3	H	Me	2-Naphthyl	DIPEA	91	90 (64)
4	H	Me	2-Naphthyl	—	<40	*rac* (*rac*)
5	H	Me	2-(MeO)C_6H_4	DIPEA	80	30 (20)
6	H	Me	2-(MeO)C_6H_4	—	<40	40 (20)
7	H	Me	3-Pyridyl	DIPEA	73	96 (92)
8	H	Me	3-Pyridyl	—	73	96 (96)
9	H	Me	4-MeC_6H_4	DIPEA	91	88 (96)
10	H	Me	4-MeC_6H_4	—	67	99 (92)

[a] The *endo:exo* ratio was always >98:2 (^{1}H NMR spectroscopy, and chiral HPLC). [b] Isolated after flash chromatography. [c] In brackets the result obtained previously with (*S*)-Binap-AgTFA complex. [d] Determined by chiral HPLC of the crude product. Identical *ee* was determined after purification.

References

1. Karoyan P, Sagan S, Lequin O, Quancard J, Lavielle S, Chassaing G (2004) Substituted Prolines Syntheses and Applications en Structure-Activity Relationship Studies of Biologically Active Peptides. In: Attanasi, OA, Spinelli, D (eds) Targets in Heterocyclic Systems, vol 8. RSC, Cambridge, p 216.
2. Calaza MI, Cativiela C (2008) Eur J Org Chem 3427.
3. Companyó X, Alba AN, Ríos R (2009) Enantioselective Synthesis of Pyrolidines and Piperidines. In: Attanasi, OA, Spinelli, D (eds) Targets in Heterocyclic Systems, vol 13. RSC, Cambridge, p 147.
4. Pellisier H (2010). In Recent Developments in Asymmetric Organocatalysis. RSC, Cambridge.
5. Reetz M, List B, Jaroch S, Weinmann R (eds) (2010). Organocatalysis. Springer New York.

6. Nájera C, Sansano JM (2009) Org Biomol Chem 7:4567.

7. Nájera C, Sansano JM (2007) Chem Rev 107:4584.

8. Hüisgen R (1963) Angew Chem Int Ed 10:565

9. For recent reviews, see: a) Padwa A, Pearson WH (eds) (2003). In Synthetic Applications of 1,3-Dipolar Cycloaddition Chemistry Towards Heterocycles and Natural Products. John Wiley & Sons, New Jersey; b) Nair V Suja, TD (2007) Tetrahedron 63:12247; c) Padwa A, Bur SK (2007) Tetrahedron 63:5341; d) Pellissier H (2007) Tetrahedron 63:3235.

10. For recent reviews, see: a) Nájera C, Sansano JM (2003) Curr. Org. Chem. 7:1105; b) Nájera C, Sansano JM (2005) Angew Chem 44:6272; c) Husinec S, Savic V (2005) Tetrahedron: Asymmetry 16: 2047; d) Pandey G, Banerjee P, Gadre SR (2006) Chem Rev 106:4484; e) Pinho e Melo TMVD (2006) Eur J Org Chem 2873; f) Bonin M, Chauveau A, Micouin L (2006) Synlett 2349; g) Nájera C, Sansano JM (2008) Enantioselective Cycloadditions of Azomethine Ylides. In Hassner A (ed) Topics in Heterocyclic Chemistry, Springer, New York 12:117; h) Stanley LM, Sibi MP (2008) Chem Rev 108:2887; i) Álvarez-Corral M, Muñoz-Dorado M, Rodríguez-García I (2008) Chem Rev 108:3174; j) Naodovic M, Yamamoto H

(2008) Chem Rev 108:3132; k) Nájera C, Sansano JM, Yus M (2010) J Braz Chem Soc 21:377.

11. a) Garner P, Hu J, Parker CG, Youngs WJ, Medvetz D (2007) Tet Lett 48:3867; b) Chinchilla R, Falvello LR, Galindo N, Nájera C (2001) Eur J Org Chem 3133; c) Sebahar PR, Williams RM (2000) J Am Chem Soc 122:5666; d) Anslow AS, Harwood LM, Phillips H, Lilley IA (1995) Tetrahedron Asymmetry 6:2465.
12. Grigg R, Thornton-Pett M, Xu J, Xu LH (1999) Tetrahedron 55:13841.
13. Kanemasa S, Hayashi T, Tanaka J, Yamamoto H, Sakurai T (1991) J Org Chem 56:4473.
14. Zubía A, Mendoza L, Vivanco S, Aldaba E, Carrascal T, Lecea B, Arrieta A, Zimmerman T, Vidal-Vanaclocha F, Cossio FP (2005) Angew Chem Int Ed 44:2903.
15. Williams RM, Fegley GJ (1992) Tetrahedron Lett 33:6755; b) Alcaraz C, Fernandez MD, de Frutos MP, Marco JL, Bernabé M (1994) Tetrahedron 50:12443; c) Pyne SG, Safaei GJ, Javidan A, Skelton BW, White AH (1988) Aust J Chem 51:137; d) Grigg R, Thornton-Pett M, Yoganathan G (1999) Tetrahedron 55:1763;

Nyerges M, Bendell D, Arany A, Hibbs DE, Coles SJ, Hursthouse MB, Groundwater PW, Meth-Cohn O (1995) Tetrahedron 61:3745.

16. a) Charlton JL, Koh K, Plourde GL (1989) Tetrahedron Lett 30:3279; b) Pham VC, Charlton JL (1995) J Org Chem 60.8051.
17. a) Nájera C, Retamosa MG, Sansano JM (2006) Tetrahedron Asymmetry 17:1985; b) Nájera C, Retamosa MG, Sansano JM, de Cózar A, Cossío FP (2007) Eur J Org Chem 5038.
18. a) Burton G, Ku TW, Carr TJ, Kiesow T, Sarisky RT, Goerke JL, Baker A, Earnshaw DL, Hofmann GA, Keenan RM, Dhanak D (2005) Bioorg Med Chem Lett 15:1553; b) Slater MJ, Amphlett EM, Andrews DM, Bravi G, Burton G, Cheasty AG, Corfield JA, Ellis MR, Fenwick RH, Fernandes S, Guidetti R, Haigh D, Hartley CD, Howes PD, Jackson DL, Jarvest RL, Lovegrove VLH, Medhurst KJ, Parry NR, Price H, Shah P, Singh OMP, Stocker R, Thommes P, Wilkinson C, Wonacott A (2007) J Med Chem 50:897.
19. Vivanco S, Lecea B, Arrieta, A, Prieto P, Morao I, Linden A, Cossío FP (2000) J Am Chem Soc 122:6078.
20. Allway P, Grigg R (1991) Tetrahedron Lett 32:5817.
21. Longmire JM, Wang B, Zhang X (2002) J Am Chem Soc 124:13400.

22. a) Chen C, Li X, Schreiber SL (2003) J Am Chem Soc 125:10174; b) Knöpfel TF, Aschwanden P, Ichikawa T, Watanabe T, Carreira EM (2004) Angew Chem Int Ed 43:5971; c) Zheng W, Zhou YG (2005) Org Lett 7:5055; d) Stohler R, Wahl F, Pfaltz A (2005) *Synthesis* 1431.

23. For copper(II)-catalysed 1,3-DC see: Oderaotoshi Y, Cheng W, Fujitomi S, Kasano Y, Minakata S, Komatsu M (2003) Org Lett 5:5043.

24. a) Zeng W, Zhou YG (2007) Tetrahedron Lett 48:4619; b) Zeng W, Chen GY, Zhou YG, Li YX (2007) J Am Chem Soc 129:750; c) Yu SB, Hu XP, Deng J, Wang DY, Duan ZC, Zheng Z (2009) Tetrahedron Asymmetry 20:621; d) Wang CJ, Xue ZY, Liang G, Lu Z (2009) Chem Commun 45:2905; e) Liang G, Tong MC, Wang CJ (2009) Adv Synth Catal 351:3101; f) Shimizu K, Ogata K, Fukuzawa SI (2010) Tetrahedron Lett 51:5068; g) Oura I, Shimizu K, Ogata K, Fukuzawa SI (2010) Org Lett 12:1752; h) Xue, ZY, Liu, TL, Lu Z, Huang H, Tao HY, Wang CJ (2010) Chem Commun 46:1727.

25. a) Gao W, Zhang X, Raghunath M (2005) Org Lett 7:4241; b) Yan XX, Peng Q, Zhang Y, Zhang K, Hong W, Hou XL, Wu YD (2006)

Angew Chem Int Ed 45:1979; c) Cabrera S, Gómez-Arrayás R, Carretero JC (2007) J Am Chem Soc 127:16394; d) Cabrera S, Gómez-Arrayás R, Martín-Matute B, Cossío FP, Carretero JC (2007) Tetrahedron 63:6587; e) López-Pérez A, Adrio J, Carretero JC (2008) J Am Chem Soc 130:10084; Herández-Toribio J, Gómez-Arrayás R, Martín-Matute, B, Carretero JC (2009) Org Lett 11:393; f) LLamas T, Gómez-Arrayás R, Carretero JC (2006) Org Lett 8:1795; g) Llamas T, Gómez-Arrayás R, Carretero JC (2007) Synthesis 950; h) Martín-Matute B, Pereira SI, Peña-Cabrera E, Adrio J, Silva AMS, Carretero JC (2007) Adv Synth Catal 349:1714; i) Shi M, Shi JW (2007) Tetrahedron Asymmetry 18:645; j) Fukuzawa S, Oki H (2008) Org Lett 10:1747; k) Wang CJ, Liang G, Xue ZY, Gao F (2008) J Am Chem Soc 130:17250; l) López-Pérez A, Adrio J, Carretero JC (2009) Angew Chem Int Ed 48:340; m) Arai T, Mishiro A, Yokoyama N, Suzuki K, Sato H (2010) J Am Chem Soc 132:5338; n) Zhang C, Yu SB, Hu XP, Wang DY, Zheng Z (2010) Org Lett 12:5542; o) Padilla S, Tejero R, Adrio J, Carretero JC (2010) Org Lett 12:5608.

26. a) Dogan O, Koyuncu H, Garner P, Bulut A, Youngs WJ, Panzner M (2006) Org Lett 8:4687; b) Saito S, Tsubogo T, Kobayashi S (2007)

J Am Chem Soc 129:5364; c) Tsubogo T, Saito S, Seki K, Yamashita Y, Kobayashi S (2008) J Am Chem Soc 130:13321; d) Gothelf A S, Gothelf KV, Hazell RG, Jørgensen KA (2002) Angew Chem Int Ed 41:4236; e) Melhado AD, Luparia M, Toste FD (2007) J Am Chem Soc 129:12638; f) Shi JW, Zhao MX, Lei ZY, Shi M (2008) J Org Chem 73:305.

27. Yamashita Y, Guo XX, Takashita R, Kobayashi S (2010) J Am Chem Soc 132:3262.

28. Robles-Machín R, Alonso I, Adrio J, Carretero JC (2010) Chem Eur J 16:5286.

29. a) Alemparte C, Blay G, Jørgensen KA (2005) Org Lett 7:4569; b) Arai S, Takahasi F, Tsuji R, Nishida A (2006) Heterocycles 67:495; c) Vicario JL, Reboredo S, Badía D, Carrillo L (2007) Angew Chem Int Ed 48:6252; d) Ibrahem I, Ríos R, Vesely J, Córdova A (2007) Tetrahedron Lett 48:6252; e) Xue MX, Zhang XM, Gong LZ (2008) Synlett 691; f) Kudryavtsev KV, Zagulyaeva AA (2008) Rus J Chem 44:378; g) Chen XH, Zhang WQ, Gong LZ (2008) J Am Chem Soc 130:5652; h) Xie J, Yoshida K, Takasu K, Takemoto Y (2008) Tetrahedron Lett 49:6910; i) Agbodjan AA, Cooley BE, Copley RCB, Corfield JA, Flanagan RC, Glover BN, Guidetti R, Haigh D,

Howes PD, Jackson MM, Matsuoka RT, Medhurst KJ, Millar A, Sharp MJ, Slater MJ, Toczko JF, Xie S (2008) J Org Chem 73:3094; j) Flanagan RC, Xie S, Millar A (2008) Org Process Res Develop 12:1307; k) Nakano M, Terada M (2009) Synlett 1670; l) Yu L, He L, Chen XH, Song J, Chen WJ, Gong LZ (2009) Org Lett 11:4946; m) Chen XH, Zhang WQ, Gong LZ (2009) J Am Chem Soc 130:5652; n) Chen XH, Wei Q, Luo SW, Xiao H, Gong LZ (2009) J Am Chem Soc 130:13819; o) Iza A, Carrillo L, Vicario JL, Badía D, Reyes E, Martínez JI (2010) Org Biomol Chem 8:2238; p) Li N, Song J, Tu XF, Liu B, Chen XH, Gong LZ (2010) Org Biomol Chem 8:2016.

30. Polet D, Alexakis A, Tissot-Croset K, Corminboeuf C, Ditrich K (2006) Chem Eur J 12:3596.

31. a) Minnaard AJ, Feringa BL, Lefort, L, de Vries JD (2007) Acc Chem Res 40:1267; b) Teichert JF, Feringa BL (2010) Angew Chem Int Ed 49:2486.

32. a) Nájera C, Retamosa MG, Sansano JM (2008) Angew Chem Int Ed 47:6055; b) Nájera C, Retamosa MG, Sansano JM Spanish Patent Application: P200800908, May 2008; c) Nájera C, Retamosa MG,

Martín-Rodríguez, M, Sansano JM, de Cózar A, Cossío FP (2009) Eur J Org Chem 5622.

33. a) Mamula O, von Zelewsky A, Bark T, Bernardinelli G (1999) Angew Chem Int Ed 38:2945; b) Munakata M, Wen M, Suenaga Y, Kuroda-Sowa T, Maekawa M, Anahata M (2001) Polyhedron 20:2037; c) Brandys MC, Puddephatt RJ (2002) J Am Chem Soc 124:3946; d) Reger DL, Semeniuc R F, Elgin JD, Rassolov V, Smith MD (2006) Cryst. Growth Des. 6:2758.

34. Agbodjan AA, Cooley BE, Copley RCB, Corfield JA, Flanagan RC, Glover BN, Guidetti R, Haigh D, Howes PD, Jackson MM, Matsuoka RT, Medhurst KJ, Millar A, Sharp MJ, Slater MJ, Toczko JF, Xie S (2008) J Org Chem 73:3094.

35. a) Nájera C, Retamosa MG, Sansano JM (2007) Org Lett 9:4025; b) Nájera C, Retamosa MG, Sansano JM, de Cózar A, Cossío FP (2008) Tetrahedron: Asymmetry 19:2913.

36. Momiyama N, Yamamoto H (2004) J Am Chem Soc 126:5360.

37. Martín-Rodríguez M, Nájera C, Sansano JM, Costa PRR, Crizanto-de Lima E, Dias AG (2010) 962.

38. Martín-Rodríguez M, Nájera C, Sansano JM, Wu FL (2010) Tetrahedron: Asymmetry 21:1184 and corringendum 21:2559.

39. Wheaton CA, Jennings MC, Puddephatt RJ (2009) Z Naturforsch 64b:1469.

40. For recent reviews about multifunctional catalysis, see: a) Ma JM, Cahard D (2004) Angew Chem Int Ed 43:4566; b) Kanai M, Kato N, Ichikawa E, Shibasaki M (2005) Pure Appl Chem 77:2047-2052; c) Kanai M, Kato N, Ichikawa E, Shibasaki M (2005) Synlett 1491; d) Shibasaki M, Kanai M, Matsunaga S (2006) Aldrichimica Acta 39:31; e) Walsh PJ, Kozlowski MC (2009). Fundamentals of Asymmetric Catalysis. University Science Books, New York.

41. Unpublished results.